Chapter 4

Physics fundamentals

The ocean circulates, redistributing heat, carbon and tracers over the globe. This advective transfer can be seen in how seaweed, floating debris and sediments are swept along the shoreline, as well as on a grander scale in how warm water is moved from the tropics for thousands of kilometres by the ocean before releasing its warmth to the atmosphere. Currents occur in a range of guises: as narrow, fast jets; meandering boundary currents; spinning vortices and vibrant eddies; as well as broad and weak interior flows.

Ocean currents are mainly driven by the frictional drag from the wind blowing over the sea and the air–sea exchange of heat and fresh water. While this forcing is comparatively easy to understand, the ocean's response is more complex. The crucial point to grasp is that the ocean flows take a long time to move any significant distance over the globe and, during that time, the spinning Earth completes many rotations around its axis; for example, even for fast currents, like the Gulf Stream moving at over $1\,\mathrm{m\,s^{-1}}$, the Earth completes 10 rotations in the time a water parcel takes to travel 1000 km. Consequently, the effects of the Earth's rotation need to be considered in order to understand the motion of any ocean current lasting a day or longer.

In this chapter, we explain how the ocean circulates, responding to accelerations on a rotating planet, in a broadly descriptive manner; accompanying mathematical expressions are summarised in boxes. The physical balances are used to define the different parts of the circulation and relate the interior circulation to the density distribution. Finally, we describe the patterns of atmospheric forcing, mapping out the variations in wind stress and air–sea fluxes of heat and fresh water over the globe.

4.1 Which forces are important for the ocean circulation?

In order to understand the ocean circulation, it is important to understand how fluid is accelerated by forces. Let's start by considering the external forces and then move onto the apparent forces arising from the Earth's rotation; accompanying mathematical derivations are provided in Appendix A.2.

4.1.1 What are the external forces?

Intuitively, one can expect there to be several forces that are important for a fluid:

- Gravity always acts to accelerate masses towards each other, whether it is raindrops falling towards the ground, water cascading in a breaking wave on the seashore or the orbital movement of the Moon around the Earth. The gravitational acceleration is independent of the mass of the object and, for the Earth, varies inversely with the square of the distance from the centre of the Earth. The gravitational force on an object is then its mass multiplied by the gravitational acceleration.
- Pressure contrasts affect the flow. For fluids, the pressure is defined as the force per unit area against a normal surface, where the force is given by the weight of the overlying fluid. Not

P1: SFK Trim: 246mm × 189mm Top: 7.5mm Gutter: 20mm
CUUK1441-04 CUUK1441/Williams 978 0 521 84369 0 May 20, 2011 20:34

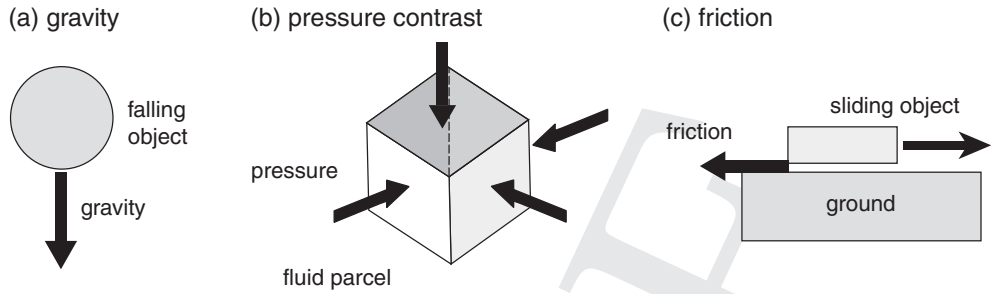

Figure 4.1 A schematic figure denoting examples of external forces: (a) gravity provides a downward acceleration (black arrow) on a falling object towards the Earth; (b) pressure contrasts acting on a parcel of fluid, the pressure (black arrow) is directed inwards on each face of the parcel; and (c) friction (black thick arrow) acts to oppose the movement of an object sliding over the ground.

surprisingly, pressure increases with depth in the ocean, such that if a metal can is dropped in the ocean, the can becomes compressed and crushed as it falls to greater depths and the overlying weight of water becomes greater. Fluid motion depends on the contrast in pressure, such that fluid is accelerated from high to low pressure.

- A frictional force can act either to decelerate moving objects, such as when a book slides across a table or water moves near the sea floor, or conversely to accelerate the flow, such as when the wind blows over a calm lake, exciting waves and the movement of water.

In summary, we expect a fluid to be accelerated (i) by gravity towards a large mass, (ii) from high to low pressure, and (iii) in the direction of a frictional acceleration.

In most everyday situations, these forces are sufficient to explain the motion of a fluid. However, additional forces need to be taken into account to understand the motion on the spinning Earth; these additional forces are important whenever the motion persists long enough for the Earth to rotate a significant distance about its own axis.

4.1.2 What is the effect of rotation?

To understand the effect of rotation, consider an everyday situation of three children playing with a ball in a park, where two of the children, A and C, are standing on the ground in the park, while the other child B is on a spinning merry-go-round (Fig. 4.2a).

Consider what is seen when a ball is thrown from child A to C. From their perspective, there are no surprises: the ball moves in a straight line from A to C (Fig. 4.2b), consistent with our intuition. However, child B sitting on the spinning merry-go-round sees a completely different picture: the ball instead appears to move in a curved path, its velocity changing direction and so being accelerated during its flight (Fig. 4.2c). The apparent acceleration of the moving ball is a consequence of the rotation of the merry-go-round: if the merry-go-round spins in an anticlockwise sense, the moving ball appears to be deflected in a clockwise direction; while if the merry-go-round spins in a clockwise sense, then the ball appears to be deflected in an anticlockwise direction; finally, if the merry-go-round spins faster, then there is a larger apparent deflection.

For the child watching in the rotating frame, there is a real problem in understanding why the ball appears to follow a curved path. During the flight of the ball, no external forces are acting to deflect the horizontal velocity; gravity simply makes the ball fall towards the ground, air resistance slows the ball down, but does not deflect the ball into a curved path, and pressure contrasts in the air are relatively unimportant for the moving ball. Instead, for the child in the rotating frame, the trajectory of the ball can only be explained by invoking *apparent accelerations*, which take into account the rotation of the merry-go-round.

The apparent acceleration of the ball (as seen by the child on the merry-go-round) is made up of two contributions:

P1: SFK Trim: 246mm × 189mm Top: 7.5mm Gutter: 20mm
CUUK1441-04 CUUK1441/Williams 978 0 521 84369 0 May 20, 2011 20:34

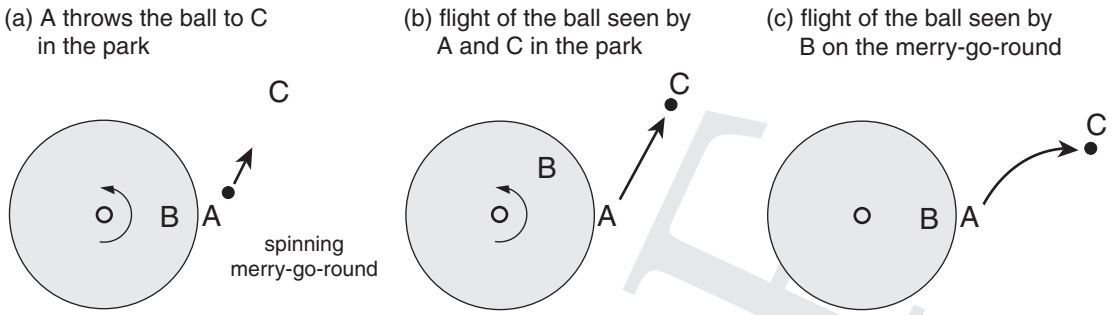

Figure 4.2 A schematic figure depicting why there are apparent accelerations. Consider three children playing with a ball in a park with children A and C standing on the ground and child B on a spinning merry-go-round (grey): (a) initially, A throws a ball towards C and at that instant A and B are alongside each other; while at a later time, (b) and (c), A sees the ball move in a straight line to C (while at the same time, B moves away from A), but conversely, B on the merry-go-round sees the ball moves in a curved path to C.

- The centrifugal acceleration provides an outward acceleration, depending on the distance of the ball from the rotational axis and the rotation rate of the merry-go-round (but is independent of the ball's velocity). This acceleration is always outward, irrespective of which way the merry-go-round spins.
- The Coriolis acceleration, which depends on the velocity of the ball and the rotation rate of the merry-go-round, provides a deflection perpendicular to the velocity of the ball. This deflection is to the right of its motion when the merry-go-round rotates in an anticlockwise sense and to the left when the merry-go-round rotates in a clockwise sense.

Hence, the child in the rotating frame sees the ball accelerated outward by the centrifugal acceleration and deflected perpendicular to its motion by the Coriolis acceleration.

In a similar manner, an observer on the spinning Earth sees the effects of these apparent accelerations for any moving particles. In most everyday situations, the motion usually only persists for a short time and the apparent deflections are not noticeable. However, if the motion lasts for a day or more, then the moving particles appear to be deflected in the same manner as in the merry-go-round example; for a derivation of the apparent accelerations, see Appendix A.2.2.

4.1.3 What are the balances of the forces?

When viewed from the rotating Earth, the atmosphere or ocean is accelerated by a combination of external forces consisting of gravity, pressure contrasts and friction, as well as by the two apparent accelerations, Coriolis and centrifugal (Box 4.1). To begin with this system appears to be rather difficult to understand, but thankfully in many situations only a few of the forces dominate and for practical purposes can be grouped together:

- In the horizontal plane, the dominant forces are from horizontal pressure contrasts and the apparent Coriolis acceleration, together with frictional stresses near boundaries.
- In the vertical plane, the dominant forces are from gravity and the vertical pressure gradient. The apparent centrifugal acceleration also plays a minor role, deforming the shape of the Earth, which is accommodated by the gravitational acceleration, g, varying with latitude (Appendix A.2.2).

4.2 How is the surface circulation determined?

Given the forces acting on the ocean, now consider how the surface circulation is determined in relation to observational diagnostics. The surface circulation is revealed by drifters spreading at a typical depth of 15 m over the North Atlantic (Fig. 4.3), highlighting the intense western boundary current, as well as the weaker, broadly clockwise circulation over the basin interior. This surface circulation involves a complicated response

P1: SFK Trim: 246mm × 189mm Top: 7.5mm Gutter: 20mm
CUUK1441-04 CUUK1441/Williams 978 0 521 84369 0 May 20, 2011 20:34

Box 4.1 The momentum equations

Newton's second law, force equals mass times acceleration, $F = ma$, is used to relate the rate of change of velocity in a fluid to accelerations from gravity, the pressure gradient, friction, Coriolis and centrifugal (derived in Appendix A.2):

$$\frac{Du}{Dt} + 2\Omega w\cos\phi - 2\Omega v\sin\phi + \frac{1}{\rho}\frac{\partial P}{\partial x} = \mathcal{F}_x \quad (4.1a)$$

$$\frac{Dv}{Dt} + 2\Omega u\sin\phi + \frac{1}{\rho}\frac{\partial P}{\partial y} = \mathcal{F}_y \quad (4.1b)$$

$$\underbrace{\frac{Dw}{Dt}}_{\text{local acceleration}} \underbrace{+ g}_{\text{gravity and centrifugal}} \underbrace{- 2\Omega u\cos\phi}_{\text{Coriolis}} + \underbrace{\frac{1}{\rho}\frac{\partial P}{\partial z}}_{\text{pressure gradient}} = \underbrace{\mathcal{F}_z}_{\text{friction}} \quad (4.1c)$$

where the velocity ($\mathrm{m\,s^{-1}}$) is separated into components u, v and w in the eastward x, northward y and vertical z directions; D/Dt represents the rate of change following the flow ($\mathrm{s^{-1}}$), g represents the gravitational acceleration ($\mathrm{m\,s^{-2}}$) including the attraction of masses to each other and a weaker contribution from the centrifugal acceleration, $\Omega = 2\pi/\text{day}$ is the angular velocity of the Earth ($\mathrm{s^{-1}}$), ϕ is latitude, P is pressure ($\mathrm{N\,m^{-2}} = \mathrm{kg\,m^{-1}\,s^{-2}}$), ρ is density ($\mathrm{kg\,m^{-3}}$) and $\mathcal{F}$ represents the frictional acceleration ($\mathrm{m\,s^{-2}}$).

For large-scale ocean and atmospheric flows, there are two important simplifying approximations to these momentum equations:

(a) The vertical velocity is relatively small compared with the horizontal velocity, such that terms involving w can be ignored ($2\Omega w\cos\phi$ and Dw/Dt). In the vertical component, the dominant remaining terms in (4.1c) lead to a hydrostatic balance,

$$\frac{\partial P}{\partial z} = -\rho g, \quad (4.2)$$

with the vertical pressure gradient balancing the gravitational acceleration.

(b) The slowness of the large-scale motion leads to the local accelerations, Du/Dt and Dv/Dt, being relatively small, so that there is a three-way balance between the Coriolis acceleration, the horizontal pressure gradient and frictional acceleration in (4.1a,b) in the horizontal plane,

$$-fv + \frac{1}{\rho}\frac{\partial P}{\partial x} = \frac{1}{\rho}\frac{\partial \tau_x}{\partial z}, \quad (4.3a)$$

$$fu + \frac{1}{\rho}\frac{\partial P}{\partial y} = \frac{1}{\rho}\frac{\partial \tau_y}{\partial z}, \quad (4.3b)$$

where the Coriolis parameter is $f \equiv 2\Omega\sin\phi$ in $\mathrm{s^{-1}}$ and the frictional acceleration is written in terms of a vertical gradient of a frictional stress, τ ($\mathrm{N\,m^{-2}}$).

P1: SFK Trim: 246mm × 189mm Top: 7.5mm Gutter: 20mm
CUUK1441-04 CUUK1441/Williams 978 0 521 84369 0 May 20, 2011 20:34

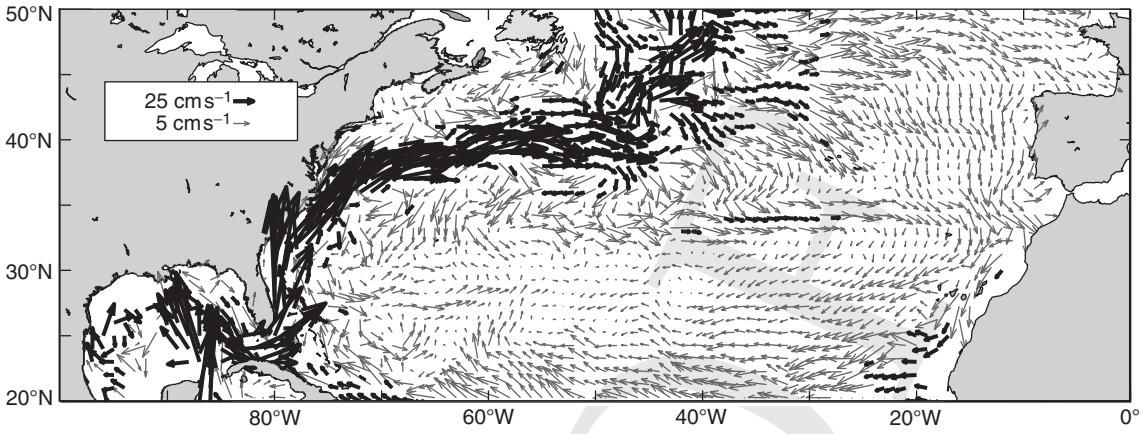

Figure 4.3 Time-mean velocity of surface drifters (cm s^{-1}) in the subtropical North Atlantic from October 1989 to April 2004: a separate scale is used for velocities exceeding 10 cm s^{-1} with velocities greater or less than 10 cm s^{-1} denoted by dark or light vectors, respectively. Courtesy of Rick Lumpkin; for full details of these Lagrangian measurements, see Lumpkin and Pazos (2006).

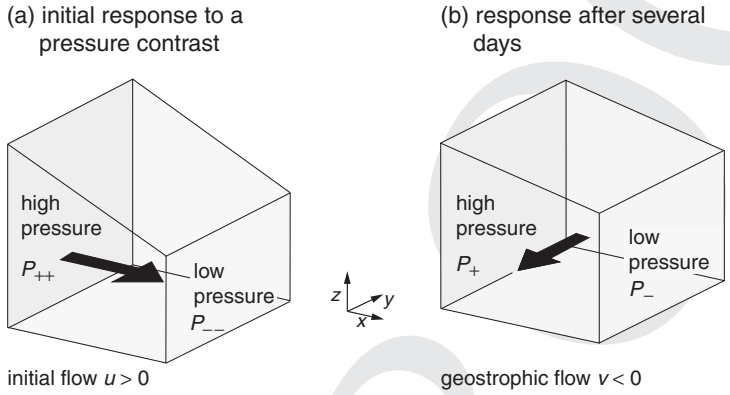

Figure 4.4 A schematic figure displaying (a) the initial response to a pressure contrast within a fluid (represented by a different thickness in the fluid), where the flow moves from high to low pressure and this redistribution of mass acts to reduce the pressure contrasts; (b) the counterintuitive response after a day or longer, where the flow is directed parallel to the pressure contours with high pressure to the right in the northern hemisphere. This flow along the pressure contours is referred to as the geostrophic flow.

to the action of the surface wind stress and horizontal pressure gradient, which is constrained by the rotation of the planet. Accordingly, the surface circulation can be separated into different components, each defined by their own dynamical balance: a geostrophic component related to a balance between the Coriolis acceleration and pressure gradient; and an Ekman component related to a balance between the Coriolis acceleration and the effect of the wind stress. Now consider each of these components in turn.

4.2.1 Geostrophic balance

Start by considering how water flows in response to a pressure contrast, such as formed by water piling up on one side of a bath or ocean basin. After this pressure contrast is created, the water naturally responds by starting to move from high to low pressure (Fig. 4.4a). Within a bath, this adjustment takes a few seconds and the water surface quickly becomes flat, the pressure contrast disappears and the flow ceases.

Within the ocean, the adjustment process usually takes much longer, requiring perhaps many days for the water to move from a region of high to low pressure. Consequently, when viewed from the rotating Earth, the moving water appears to become deflected by an apparent acceleration, the Coriolis acceleration, directed to the right of flow in the northern hemisphere and to the left in the southern hemisphere (as in the merry-go-round example in Fig. 4.2). This deflection then leads to the water moving parallel to pressure contours (Fig. 4.4b), rather than moving from high to low pressure; the same balance occurs in the atmosphere with air moving along pressure contours.

P1: SFK Trim: 246mm × 189mm Top: 7.5mm Gutter: 20mm
CUUK1441-04 CUUK1441/Williams 978 0 521 84369 0 May 20, 2011 20:34

Box 4.2 How does fluid move in response to pressure contrasts?

How fluid responds to a pressure gradient on a rotating planet can be defined in terms of the relative size of the local accelerations, Du/Dt and Dv/Dt, and the Coriolis accelerations, $-fv$ and fu, as measured by the non-dimensional Rossby number,

$$Ro \equiv \frac{U}{fL}, \tag{4.4}$$

where U is the typical magnitude of the horizontal velocity, L is the typical horizontal length scale and f is the Coriolis parameter. To understand the different regimes, for simplicity, assume that frictional accelerations are neglected.

(a) For most everyday situations, such as throwing a ball in a park or water moving in a bath, the motion lasts only for a few seconds and the Coriolis acceleration from the Earth's rotation is unimportant (as the Earth has not rotated far in such a short time); this regime is defined by the Rossby number being large, $Ro \gg 1$. In this case, the Coriolis acceleration is relatively small and the horizontal momentum equations (4.1a,b), with friction neglected, reduce to

$$\frac{Du}{Dt} + \frac{1}{\rho}\frac{\partial P}{\partial x} \simeq 0,$$

$$\frac{Dv}{Dt} + \frac{1}{\rho}\frac{\partial P}{\partial y} \simeq 0,$$

and fluid is accelerated from high to low pressure.

(b) For timescales of a day or longer, the Coriolis acceleration becomes important due to the significant rotation of the Earth during that time; this regime is defined by the Rossby number being relatively small, $Ro \ll 1$. The horizontal momentum equations (4.1a,b), with friction neglected, instead reduce to a geostrophic balance,

$$-fv + \frac{1}{\rho}\frac{\partial P}{\partial x} \simeq 0,$$

$$fu + \frac{1}{\rho}\frac{\partial P}{\partial y} \simeq 0,$$

where fluid moves along pressure contours (high P to right of motion where $f > 0$), rather than from high to low pressure. This geostrophic balance is used to infer the large-scale circulation from the pressure field.

This geostrophic velocity is defined by this balance between the pressure gradient and Coriolis acceleration (Box 4.2), as given by

$$u_g = -\frac{1}{\rho f}\frac{\partial P}{\partial y}, \tag{4.5a}$$

$$v_g = \frac{1}{\rho f}\frac{\partial P}{\partial x}, \tag{4.5b}$$

where u_g and v_g are the eastward and northward geostrophic velocities ($\mathrm{m\,s^{-1}}$), ρ is density ($\mathrm{kg\,m^{-3}}$) and P is the pressure ($\mathrm{N\,m^{-2}}$). The Coriolis parameter is defined by $f = 2\Omega \sin\phi$ in $\mathrm{s^{-1}}$, where $\Omega = 2\pi/\mathrm{day}$ is the angular velocity and ϕ is the latitude: f increases poleward with latitude, ranging from 2Ω at the North Pole, 0 at the equator and -2Ω at the South Pole. The units of (4.5a,b) are given by

$$\mathrm{m\,s^{-1}} = \frac{\mathrm{N\,m^{-2}}}{(\mathrm{kg\,m^{-3}})(\mathrm{s^{-1}})(\mathrm{m})},$$

P1: SFK Trim: 246mm × 189mm Top: 7.5mm Gutter: 20mm
CUUK1441-04 CUUK1441/Williams 978 0 521 84369 0 May 20, 2011 20:34

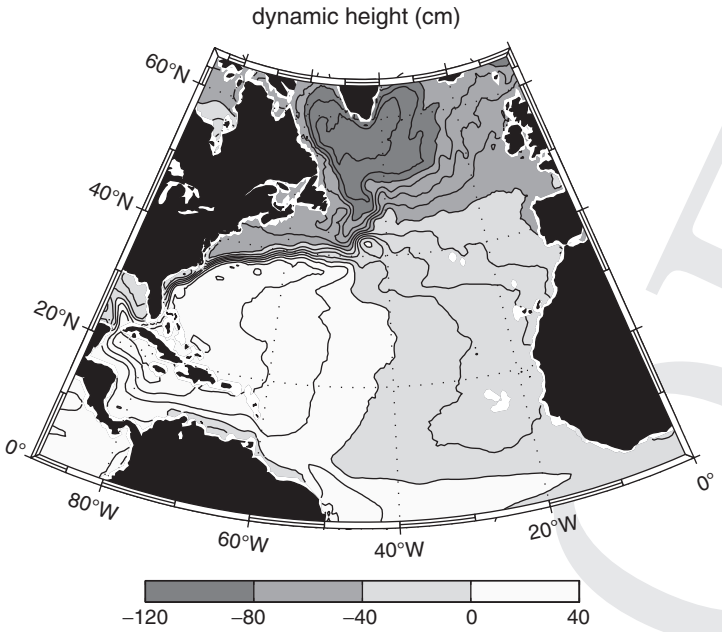

Figure 4.5 Map of dynamic height (contours with an interval of 10 cm) for the North Atlantic (with a Lambert projection). The surface geostrophic flow is aligned along dynamic height contours with high dynamic height to the right of the motion in the northern hemisphere. Ocean mean dynamic height was taken from a combined dataset integrating information from surface drifters, satellite altimetry, surface winds and the GRACE gravity mission (Niiler *et al.*, 2003; Maximenko and Niiler, 2005).

which are equivalent (remembering $\mathrm{N} \equiv \mathrm{kg\,m\,s^{-2}}$).

The geostrophic flow is directed along pressure contours with high pressure to the right of the motion in the northern hemisphere and reversing to the left of the motion in the southern hemisphere. For example, in the northern hemisphere, there is an eastward geostrophic flow when pressure decreases northward, $\partial P/\partial y < 0$, and a southward geostrophic flow when pressure decreases eastward, $\partial P/\partial x < 0$ (Fig. 4.4b); in both these cases, high pressure is to the right of the flow. This geostrophic flow represents the dominant contribution to the time-mean velocity of the surface drifters in Fig. 4.3.

Dynamic height

For the ocean, the geostrophic flow (4.5a,b) can equivalently be defined in terms of the horizontal gradient in dynamic height, η, in m:

$$u_g = -\frac{g}{f}\frac{\partial \eta}{\partial y},$$

$$v_g = \frac{g}{f}\frac{\partial \eta}{\partial x},$$

where the dynamic height represents the vertical displacement of a pressure surface above a reference surface called the geoid (a surface of constant gravitational acceleration).

Geostrophic currents flow along contours of dynamic height with higher dynamic height to the right of the flow in the northern hemisphere. For example, a map of dynamic height over the North Atlantic (Fig. 4.5) reveals the broadly clockwise circulation over the mid latitudes (10°N to 40°N) changing to an anticlockwise circulation at higher latitudes (40°N to 65°N). The flow strengthens when contours of dynamic height are closely spaced, as occurring along the Gulf Stream and its extension into the basin (30°N to 40°N).

4.2.2 Ageostrophic and Ekman flow

While the ocean circulation is often close to the geostrophic flow, there are other contributions to the flow, collectively referred to as ageostrophic flow (denoted by subscript ag) as defined by the difference between the actual flow and the geostrophic flow:

$$u = u_g + u_{ag},$$

$$v = v_g + v_{ag}.$$

The ageostrophic contributions are associated with frictional acceleration and local accelerations; these ageostrophic contributions can

P1: SFK Trim: 246mm × 189mm Top: 7.5mm Gutter: 20mm
CUUK1441-04 CUUK1441/Williams 978 0 521 84369 0 May 20, 2011 20:34

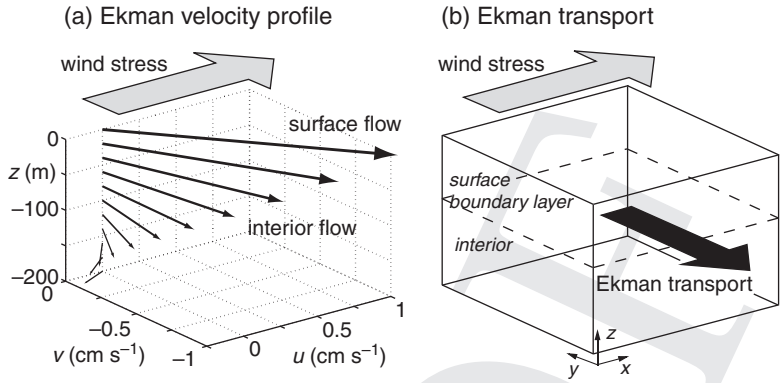

Figure 4.6 The effect of the wind stress on the interior flow: (a) the Ekman velocity rotates and weakens with depth. Theory suggests that the surface velocity is at 45° to the right of the wind stress and spirals in a clockwise manner in the northern hemisphere; (b) the surface stress drives a horizontal Ekman transport within a thin surface boundary layer, directed to the right of the wind in the northern hemisphere. In (a), the velocity profile is calculated for an eastward wind stress, $\tau_x^s = 0.1\,\mathrm{N\,m^{-2}}$, and an interior stress assumed to follow $\tau = \rho A_v \partial \mathbf{u}/\partial z$ with a constant eddy viscosity, $A_v = 0.5\,\mathrm{m^2\,s^{-1}}$ and $f = 10^{-4}\,\mathrm{s^{-1}}$, using $u(z) = u_0 e^{z/d}\cos(z/d - \pi/4)$ and $v(z) = u_0 e^{z/d}\sin(z/d - \pi/4)$ with $u_0 = \sqrt{2}\tau_x^s/(\rho f d)$ and $d = (2A_v/f)^{1/2}$ is taken as the thickness of the Ekman layer; see Vallis (2006) for further details of the analytical solution.

equivalently be defined by the terms in (4.1a,b) which have been neglected in forming the geostrophic balance (4.5a,b). The most important ageostrophic contribution involves the frictional acceleration imparted at the boundary, involving either a wind stress from air moving over the ocean or a bottom stress from fluid moving over the sea floor.

Focussing on the surface ocean, the wind stress at the sea surface is communicated by turbulent mixing over a thin boundary layer and drives an ageostrophic velocity, called the Ekman velocity,

$$u_{ek} = \frac{1}{\rho f}\frac{\partial \tau_y}{\partial z}, \tag{4.6a}$$

$$v_{ek} = -\frac{1}{\rho f}\frac{\partial \tau_x}{\partial z}, \tag{4.6b}$$

where u_{ek} and v_{ek} are the eastward and northward Ekman velocities, and τ_x and τ_y represent the frictional and turbulent stresses acting within the water column ($\mathrm{N\,m^{-2}}$), directed eastward and northward.

The Ekman velocity is defined by a balance between the frictional acceleration and the Coriolis acceleration (from (4.3a,b) in Box 4.1). The frictional acceleration depends on the vertical gradient in stress and drives an Ekman velocity to the right of the stress in the northern hemisphere. Assuming a simple form as to how the stress varies with depth suggests that the Ekman velocity spirals and weakens with depth (Fig. 4.6a).

The effect of this frictional deflection was first reported by Fridtjof Nansen who, while in his ship, the *Fram*, trapped in the Arctic ice, noticed how icebergs drifted 20° to 40° to the right of the wind; the mathematical description of the velocity spiral providing this drift was subsequently provided by Vagn Ekman in 1902. The details of the predicted velocity spiral (such as in Fig. 4.6a) are rarely seen though, only appearing under calm conditions under sea ice or when long time averages are applied to velocity profile measurements.

Ekman transport

While the details of the Ekman velocity profile are difficult to verify, there is a robust relationship between the wind stress and the depth integral of the Ekman velocities given by

$$U_{ek} \equiv \int_{-D}^{0} u_{ek}\,dz = \frac{\tau_y^s}{\rho f}, \tag{4.7a}$$

and

$$V_{ek} \equiv \int_{-D}^{0} v_{ek}\,dz = -\frac{\tau_x^s}{\rho f}, \tag{4.7b}$$

where U_{ek} and V_{ek} represent the Ekman volume flux per unit length, having units of $\mathrm{m^2\,s^{-1}}$ from the depth integral of velocity, and D represents the

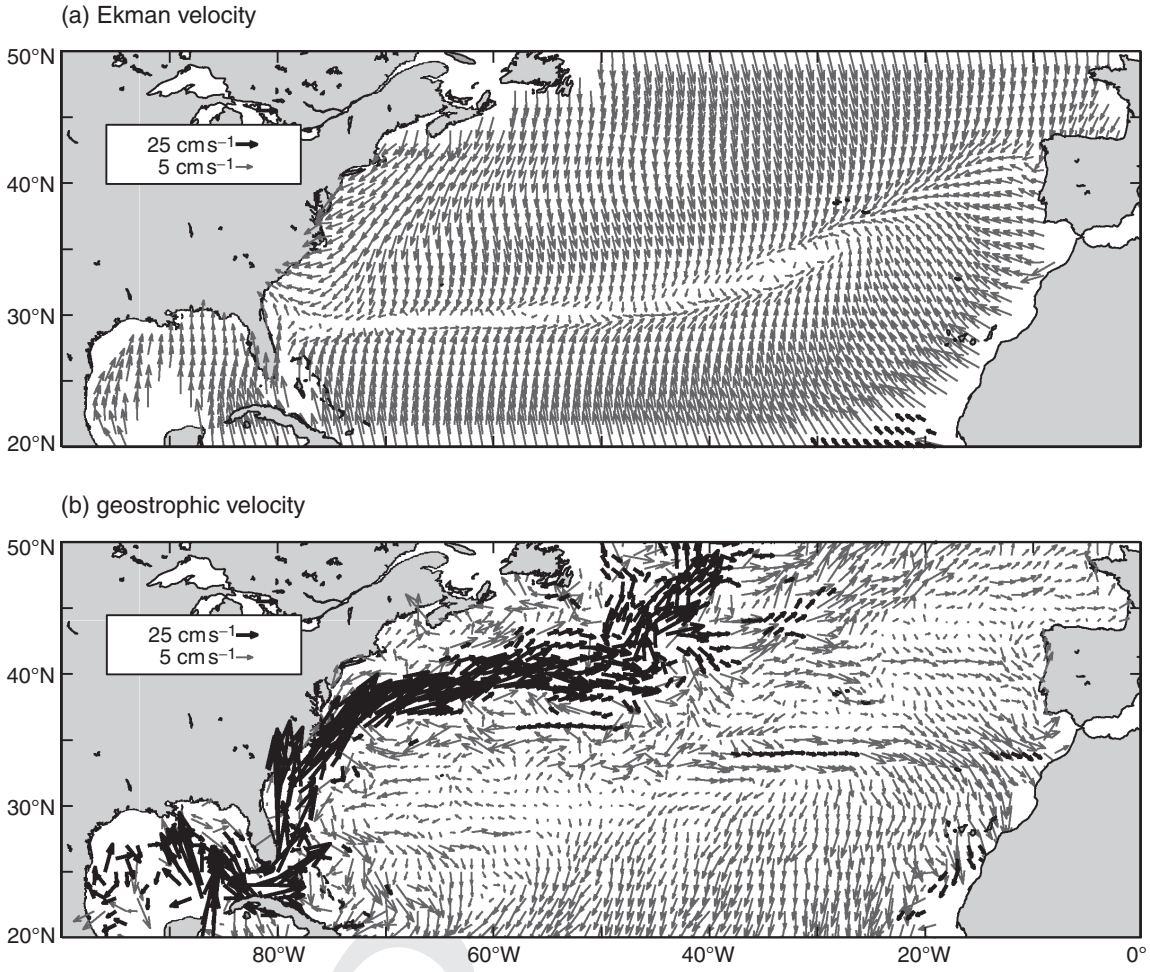

Figure 4.7 Time-mean velocity (cm s^{-1}) of surface drifters (as in Fig. 4.3) separated into (a) an Ekman component predicted from the wind stress and (b) a geostrophic component from the difference between the time-mean velocity and the Ekman velocity. Courtesy of Rick Lumpkin; for further details, see Lumpkin and Pazos (2006).

thickness of the surface boundary layer, extending from the surface to a depth of several tens of metres to 100 m. An Ekman transport in m^3 s^{-1} is then given by the horizontal integral of the Ekman volume flux, which is directed at right angles to the imposed wind stress (Fig. 4.6b): an eastward wind stress, $\tau_x^s > 0$, imparts an equatorward transport, $V_{ek} < 0$, and a northward wind stress, $\tau_y^s > 0$, imparts an eastward transport, $u_{ek} > 0$, in the northern hemisphere.

North Atlantic drifter example

Returning to the drifter trajectories over the North Atlantic (Fig. 4.3), their average velocities can be separated into Ekman and geostrophic velocity components; the Ekman component is diagnosed from the surface winds, assuming a simple form for how the stress is communicated (as in Fig. 4.6a). The Ekman drift of the drifters, as depicted in Fig. 4.7a, varies from southward along the northern flank of the subtropical gyre, where there is an eastward wind stress, to northward along its southern flank, where there is a westward wind stress. There is a stronger geostrophic velocity over much of the subtropical gyre, revealing again a clockwise circulation and an intense western boundary current (Fig. 4.7b).

Ekman upwelling along the coast

The wind stress also drives vertical motion, referred to as Ekman upwelling or downwelling:

P1: SFK Trim: 246mm × 189mm Top: 7.5mm Gutter: 20mm
CUUK1441-04 CUUK1441/Williams 978 0 521 84369 0 May 20, 2011 20:34

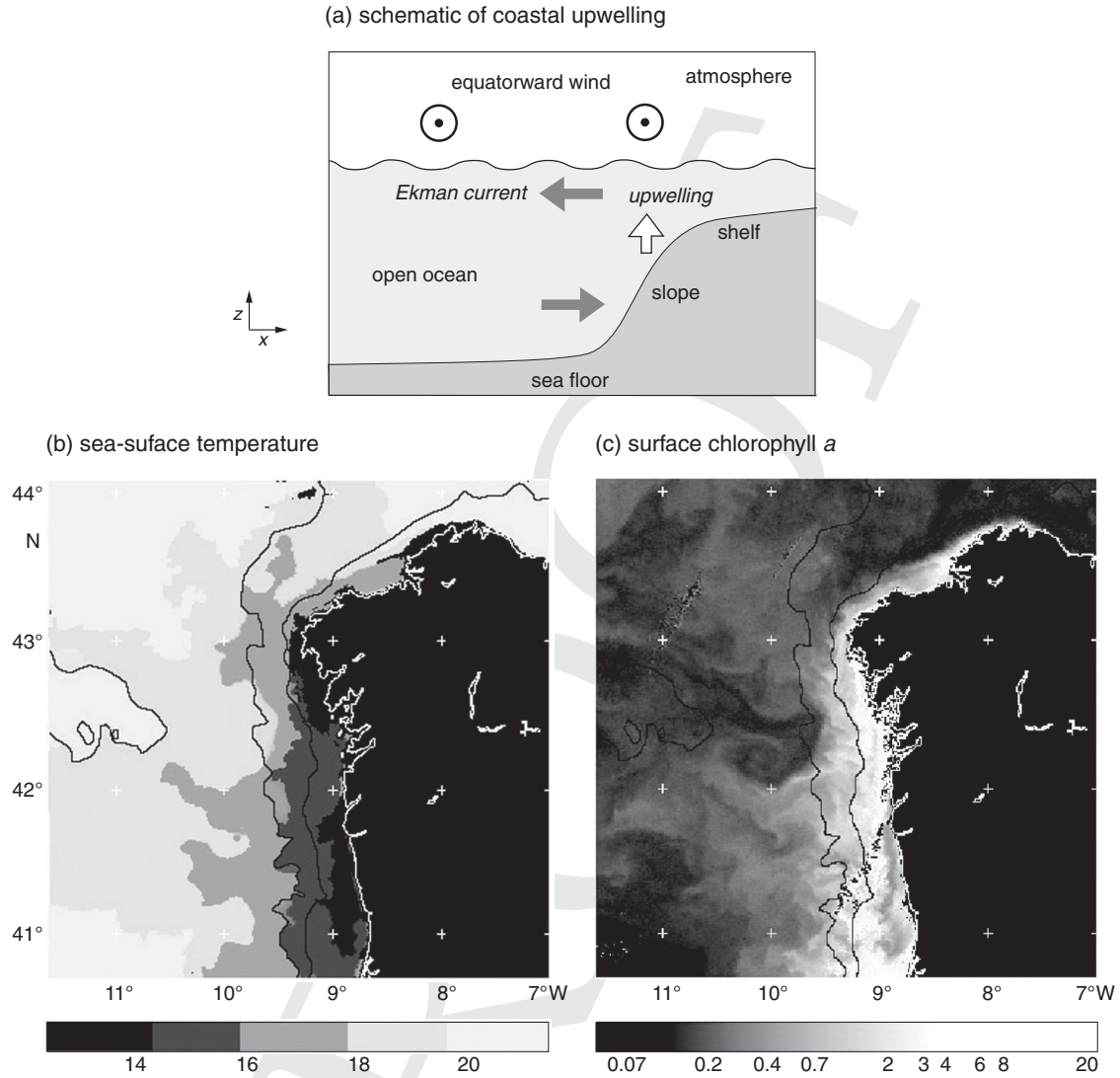

Figure 4.8 (a) A schematic figure of the Ekman upwelling; satellite pictures off Spain during an upwelling event on 3 August 1998 for (b) sea-surface temperature (°C) and (c) chlorophyll *a* (mg m^{-3}) revealing surface cold, nutrient-rich waters off the coast supporting elevated concentrations of phytoplankton. Satellite measurements courtesy of Steve Groom, NEODASS, Plymouth.

upwelling occurs whenever there is horizontal divergence, defined by when the horizontal volume flux leaving the surface boundary layer is greater than that entering (discussed further in Section 10.2.3).

This effect of the winds in driving upwelling is particularly apparent along the coast. Along an eastern boundary, an equatorward wind drives an offshore Ekman transport (Fig. 4.8a). This water swept offshore has to be supplied somehow and the only option is for cold, deep water to be upwelled along the coast; as evident in surface waters off the western coast of Spain being relatively cold and nutrient-rich and, thus, supporting high concentrations of phytoplankton (Fig. 4.8b,c). If the winds change to poleward, there is instead an onshore transport and downwelling along the eastern boundary. In a similar manner, along the western boundary, there is an offshore Ekman transport and upwelling for a poleward wind, and an onshore Ekman transport and downwelling for an equatorward wind.

Table 4.1 Variation of potential temperature, *in situ* and potential density with temperature and pressure for a salinity of 35 g kg^{-1}.

Temperature T (°C)	Pressure P (mbar)	Potential temperature θ (°C)	*In situ* density −1000 kg m^{-3} σ (kg m^{-3})	Potential density −1000 kg m^{-3} σ_θ (kg m^{-3})
20	0	20	24.8	24.8
10	0	10	27.0	27.0
5	0	5	27.7	27.7
5	2000	4.8177	36.7	27.7
5	4000	4.5828	45.4	27.7

4.3 How is the interior circulation determined?

Given how the surface flow is affected by pressure contrasts and surface stresses, now consider the deep, interior flow. Frictional stresses are confined to surface, bottom and side boundaries, so are relatively unimportant for much of the ocean interior. Instead the deeper flow is affected primarily by how the horizontal pressure gradients vary with depth, which themselves alter with changes in density. Consequently, we now consider how density and pressure vary with depth, and their relationship to the interior flow.

4.3.1 How does density vary with depth?

Density is defined as the mass per unit volume. *In situ* density, ρ, is the locally measured density and increases with increasing pressure, P, decreasing temperature, T, and increasing salinity, S (Table 4.1). The weight of overlying water compresses water at depth, increasing *in situ* density, which even reaches 1070 kg m^{-3} in the deepest part of the world's ocean, the Mariana Trench (Fig. 4.9a).

Potential density provides a pressure-corrected measure of density (Table 4.1), so at the base of the same trench, the potential density referenced to the sea surface only reaches 1028 kg m^{-3} (Fig. 4.9c). These two definitions of density serve different purposes: *in situ* density is the correct density to use when calculating the weight of the fluid, while potential density (or its more accurate relation, a neutral density surface) is the appropriate variable to employ when inferring how water masses spread (Box 4.3).

4.3.2 How does pressure vary with depth?

The weight of the overlying fluid always leads to pressure increasing with depth, as described by the hydrostatic balance (4.2),

$$\frac{\partial P}{\partial z} = -\rho g,$$

where P is in N m^{-2}, z in m, ρ in kg m^{-3} and g in m s^{-2}. This background increase in pressure with depth is by itself unimportant for the circulation, since the geostrophic flow depends on horizontal gradients in pressure.

Crucially, there is a larger pressure increase with depth in dense water than in light water, since the overlying weight is greater in dense water. Hence, horizontal gradients in density lead to horizontal gradients in pressure changing with depth.

4.3.3 How does the geostrophic flow vary with depth?

The geostrophic flow depends on horizontal pressure gradients. Given how the depth variation in pressure alters with density, the vertical shear in geostrophic velocity depends on horizontal density gradients (see Q4.2):

$$\frac{\partial u_g}{\partial z} = \frac{g}{\rho f}\frac{\partial \rho}{\partial y}, \tag{4.8a}$$

$$\frac{\partial v_g}{\partial z} = -\frac{g}{\rho f}\frac{\partial \rho}{\partial x}. \tag{4.8b}$$

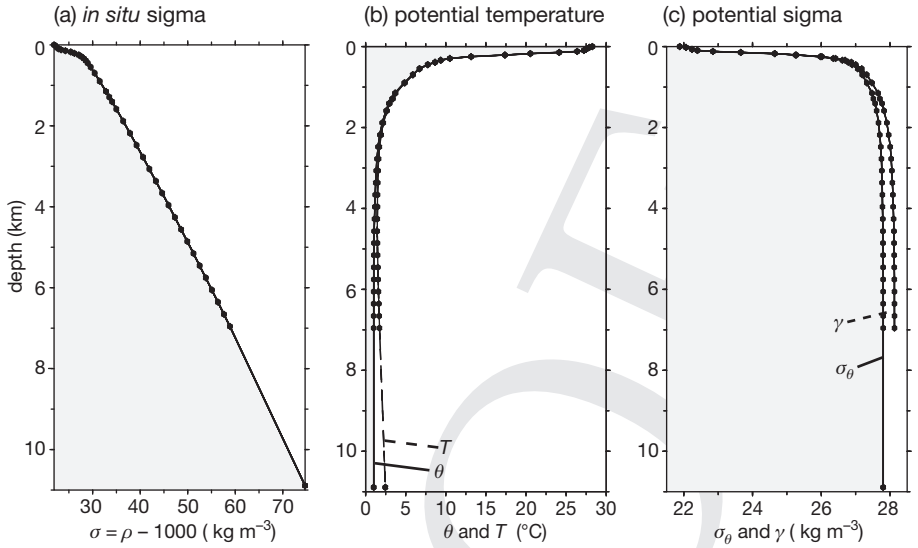

Figure 4.9 Vertical profiles of (a) *in situ* density minus 1000 kg m^{-3}, (b) potential and *in situ* temperature, θ and T (°C), and (c) potential density referenced to the sea surface minus 1000 kg m^{-3}, σ_θ, and neutral density, γ (kg m^{-3}), in the deepest part of the ocean (a depth of 10 924 m) in the Mariana Trench of the North Pacific (142.167°E, 11.333°N) evaluated from the Pacific Ocean database collated by J. L. Reid and A. W. Mantyla. The weight of overlying fluid compresses the fluid leading to an increase in the *in situ* density with depth in (a), as well as a slight increase in the *in situ* temperature with depth in (b). This adiabatic warming is accounted for by using potential temperature, θ. In (c), the vertical variations in potential density are much smaller than that of *in situ* density, taking into account the compression of water with depth. The neutral density surface, γ, usually closely follows that of potential density, differing for large depth excursions.

The units of the equation are given by

$$\frac{(\mathrm{m\,s^{-1}})}{\mathrm{m}} \sim \frac{(\mathrm{m\,s^{-2}})}{(\mathrm{kg\,m^{-3}})(\mathrm{s^{-1}})}\frac{(\mathrm{kg\,m^{-3}})}{(\mathrm{m})},$$

simplifying to s^{-1} on each side. In the northern hemisphere, a northward increase in density implies that the eastward component of the geostrophic flow becomes stronger towards the surface (4.8a), while an eastward increase in density implies that the southward component of the geostrophic flow becomes stronger towards the surface (4.8b) (Fig. 4.10). These inferred flow directions reverse in the southern hemisphere with the change in sign of the Coriolis parameter.

This balance (4.8a,b) is referred to as thermal wind, reflecting its application in the atmosphere where the vertical shear in horizontal velocity is controlled by horizontal temperature gradients, as seen in how the eastward moving Jet Stream depends on the poleward decrease in air temperature.

These vertical shear relations (4.8a,b) form the basis of historical observational attempts to infer the circulation, where the geostrophic flow at a depth z is related to that at a constant reference depth, z_{ref}, by

$$u_g(z) = u_g(z_{ref}) + \frac{g}{\rho f}\int_{z_{ref}}^{z} \frac{\partial \rho}{\partial y}\, dz, \tag{4.9a}$$

$$v_g(z) = v_g(z_{ref}) - \frac{g}{\rho f}\int_{z_{ref}}^{z} \frac{\partial \rho}{\partial x}\, dz. \tag{4.9b}$$

Thus, the geostrophic flow across a section can be inferred from a depth integration of the horizontal density gradients along the section, subject to reference velocities, $u_g(z_{ref})$ and $v_g(z_{ref})$, being either measured independently or assumed. The choice of the reference velocity only makes a slight difference to the surface velocity, but can significantly alter the volume transport when integrated with depth over the water column.

Now consider this thermal-wind method applied across the subtropical North Atlantic.

P1: SFK Trim: 246mm × 189mm Top: 7.5mm Gutter: 20mm
CUUK1441-04 CUUK1441/Williams 978 0 521 84369 0 May 20, 2011 20:34

Box 4.3 Equation of state, density and salinity

In situ density, ρ, is the locally measured density and is related to the *in situ* temperature, salinity and pressure through an empirical equation of state,

$$\rho = \rho(P, T, S), \tag{4.10}$$

where ρ increases with increasing pressure, P, decreasing temperature, T, and increasing salinity, S, as illustrated in Table 4.1; σ is used as a convenient shorthand, such that $\sigma_T = \rho - 1000\,\mathrm{kg\,m^{-3}}$. Density nearly always increases with depth, due to the increasing weight of the fluid, which slightly compresses the fluid (Fig. 4.9a). In turn, the *in situ* density alters the weight of the overlying fluid and, thus, how pressure varies with depth in (4.2).

Salinity has traditionally been defined in terms of the number of grams of salt per kilogram of seawater ($\mathrm{g\,kg^{-1}}$), as well as defined in terms of a practical salinity based on the conductivity of seawater. Absolute salinity is now the recommended choice, defined by the concentration of dissolved material in seawater in $\mathrm{g\,kg^{-1}}$, which more exactly relates to the thermodynamic properties of seawater (McDougall *et al.*, 2009).

The change in density, $\Delta\rho$, at a particular depth may be related to the change in temperature, ΔT, and salinity, ΔS, using a linearised version of the equation of state,

$$\Delta\rho/\rho = -\alpha_T \Delta T + \beta_S \Delta S, \tag{4.11}$$

where the density expansion coefficient for temperature is $\alpha_T = -\frac{1}{\rho}\frac{\partial\rho}{\partial T}$ and the density contraction coefficient for salinity is $\beta_S = \frac{1}{\rho}\frac{\partial\rho}{\partial S}$.

Potential density is a pressure-corrected density, defined as the density of a fluid parcel after moving adiabatically (without any heat exchange) from its depth to a reference depth; the corresponding σ_θ is the potential density minus $1000\,\mathrm{kg\,m^{-3}}$. Fluid parcels approximately move along potential density surfaces when there is adiabatic motion and there are limited depth changes, so this surface is useful to denote how water masses spread. However, the non-linearity of the equation of state (4.10) means that fluid parcels do not exactly follow potential density surfaces if there are large depth excursions.

Instead, fluid parcels more closely follow neutral density surfaces during adiabatic motion; these surfaces can be viewed as a continuous analogue of potential density referenced to a discrete set of reference depths (Jackett and McDougall, 1997).

Gulf Stream and North Atlantic example

Over the North Atlantic subtropical gyre, there is a westward deepening of potential density surfaces, which is particularly pronounced in the upper 1 km of the water column (Fig. 4.11). This westward decrease in density, $\partial\rho/\partial x > 0$, implies a negative velocity shear, $\partial v_g/\partial z < 0$, from (4.8b). Assuming that the deep flow is weak and approaches zero, then this vertical shear implies that the upper waters are moving southward in the interior. Conversely, along the western boundary, there is a pronounced westward shallowing of potential density surfaces, with $\partial\rho/\partial x < 0$ implying $\partial v_g/\partial z > 0$ and the upper flow is directed northward across the section.

Now estimate the northward velocity in the Gulf Stream along the western boundary from the west–east density gradient at 36°N using (4.9b),

$$\Delta v_g \sim -\frac{g}{\rho f}\frac{\Delta\rho}{\Delta x}\Delta z.$$

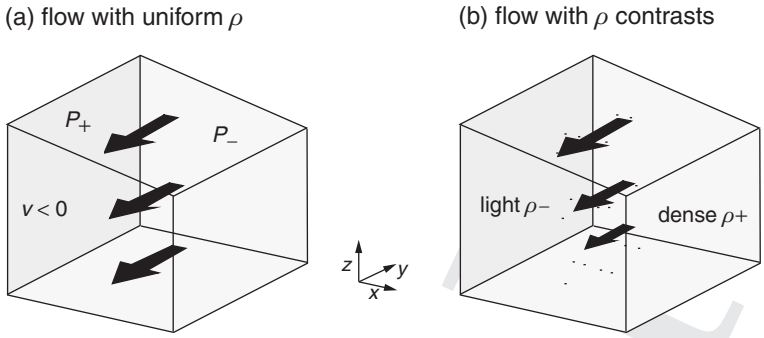

Figure 4.10 A schematic figure displaying how the geostrophic flow varies with depth for (a) uniform density where the flow and horizontal pressure gradient do not vary with depth, and (b) with a horizontal density contrast where the flow is decreasing with depth. For this example, a southward flow is depicted with surface pressure decreasing to the east and, in (b), the density is assumed to increase to the east leading to this flow weakening with depth.

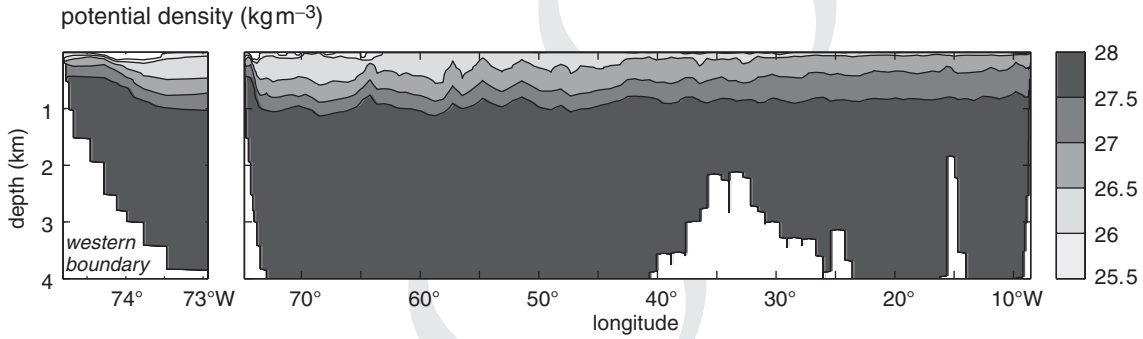

Figure 4.11 Zonal section along 36°N for potential density referenced to the sea surface, σ_θ (kg m^{-3}), in the North Atlantic in May 2005 for the western boundary (left panel) and the entire basin (right panel) over the upper 4 km. There is a general westward deepening of the isopycnals over the upper 1 km, together with a rapid shoaling along the western boundary.

Assuming a horizontal density contrast, $\Delta\rho \sim -1\,\mathrm{kg\,m^{-3}}$ over an east–west distance $\Delta x \sim 100\,\mathrm{km}$ and a depth change $\Delta z \sim 1\,\mathrm{km}$ implies a change in the northward velocity over this depth range of typically

$$\Delta v_g \sim -\frac{(10\,\mathrm{m\,s^{-2}})(-1\,\mathrm{kg\,m^{-3}})\ (10^3\,\mathrm{m})}{(10^3\,\mathrm{kg\,m^{-3}})(10^{-4}\,\mathrm{s^{-1}})(10^5\,\mathrm{m})} \sim 1\ \mathrm{m\,s^{-1}},$$

where $f \sim 10^{-4}\,\mathrm{s^{-1}}$. This northwards velocity estimate is in accord with the measured geostrophic flow reaching between 1 and 2 m s^{-1} in the surface core of the Gulf Stream (Fig. 4.12).

Volume transport

The associated meridional volume transport crossing a zonal section is given by

$$\int_{x_1}^{x_2}\int_{z_1}^{z_2} v\,dx dz,$$

where x_1, x_2 and z_1, z_2 represent the longitude and depth ranges of the integration; the units of volume transport are given by the product of velocity (m s^{-1}) with cross-sectional area (m^2), thus, volume per second (m^3 s^{-1}) and usually expressed in sverdrups (1 Sv $\equiv 10^6$ m^3 s^{-1}).

This integration can be performed in different ways to reveal either the strength of the meridional overturning circulation or the horizontal recirculation:

- The overturning is estimated if the integration is applied from the surface to a mid depth (typically 1500 m) and over the entire width of the basin. For this 36°N section in Fig. 4.11, there is a northward, upper ocean transport reaching 18 Sv, which is returned southward in the deeper ocean.
- The horizontal circulation is estimated if the integration is performed over the full depth

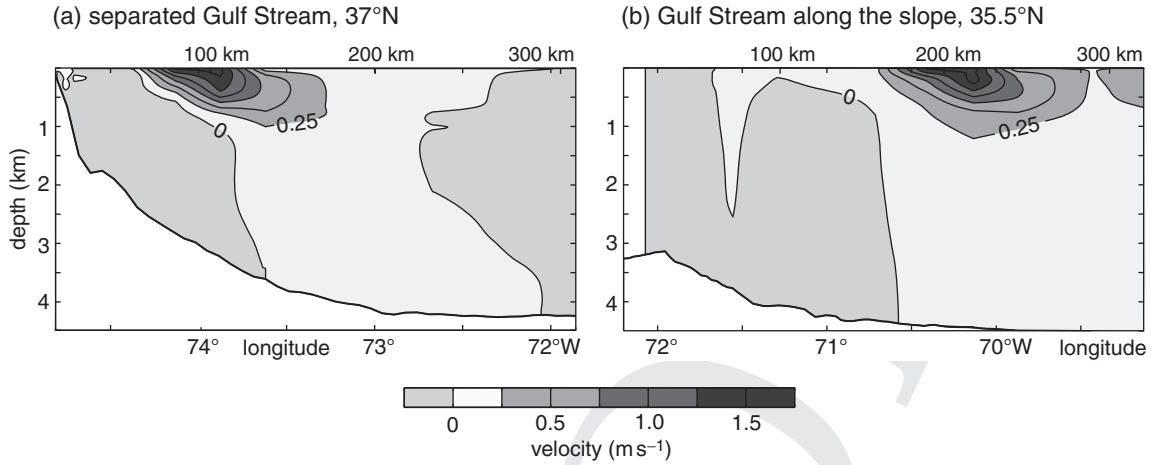

Figure 4.12 Northward geostrophic velocity ($m\,s^{-1}$) associated with (a) the Gulf Stream having separated from the coast at 37°N, and (b) the Gulf Stream running along the continental slope at 35.5°N. Data collected in May 2005; velocity data supplied by Elaine McDonagh.

range and the width of the basin interior, but excluding the western boundary. Again for the 36°N section, there is a southward, interior gyre transport reaching −50 Sv, which is returned northward as part of the Gulf Stream in the western boundary.

These transport estimates from ocean sections provide one of the key foundations of physical oceanography. There are, though, uncertainties in calculating the reference velocity and in how representative a single section is, given the seasonal and inter-annual variability in the ocean. This approach can be extended to provide the transport of associated properties, such as heat, nutrients and carbon, by melding the velocity measurements with coincident property measurements.

4.4 Global-scale patterns of atmospheric forcing

Given the preceding discussions of the physical balances in the ocean, we now return to the surface and consider the patterns of the large-scale atmospheric forcing, which ultimately drive nearly all the circulation over the globe.

4.4.1 Surface circulation and wind forcing

The atmospheric winds provide the most important forcing for the surface circulation. There is a characteristic pattern of easterly Trade winds in the tropics and westerly winds at mid latitudes (Fig. 4.13a,b). This pattern of winds provides a surface torque, a twisting force, which drives recirculations in the ocean basins between the continents, referred to as gyres, as revealed in the nearly closed contours for dynamic height (Fig. 4.13). Over the Southern Ocean, the winds provide a momentum input driving an eastward transport in the Antarctic Circumpolar Current, as revealed in the tightly spaced contours for dynamic height (with high values of dynamic height to the left of the flow).

There is a strong seasonal cycle in the surface winds: the pole–equator temperature contrast in the atmosphere is much greater in winter, leading to a stronger eastward flow in the upper atmosphere (from thermal-wind balance), with a more vigorous Jet Stream and more frequent mid-latitude storms. Accordingly, this seasonal strengthening of the winds leads to a stronger surface stress and torque being imparted to the ocean in winter, compared with in summer (Fig. 4.13a,b).

Now consider the global patterns for the surface fluxes of heat and fresh water.

P1: SFK Trim: 246mm × 189mm Top: 7.5mm Gutter: 20mm
CUUK1441-04 CUUK1441/Williams 978 0 521 84369 0 May 20, 2011 20:34

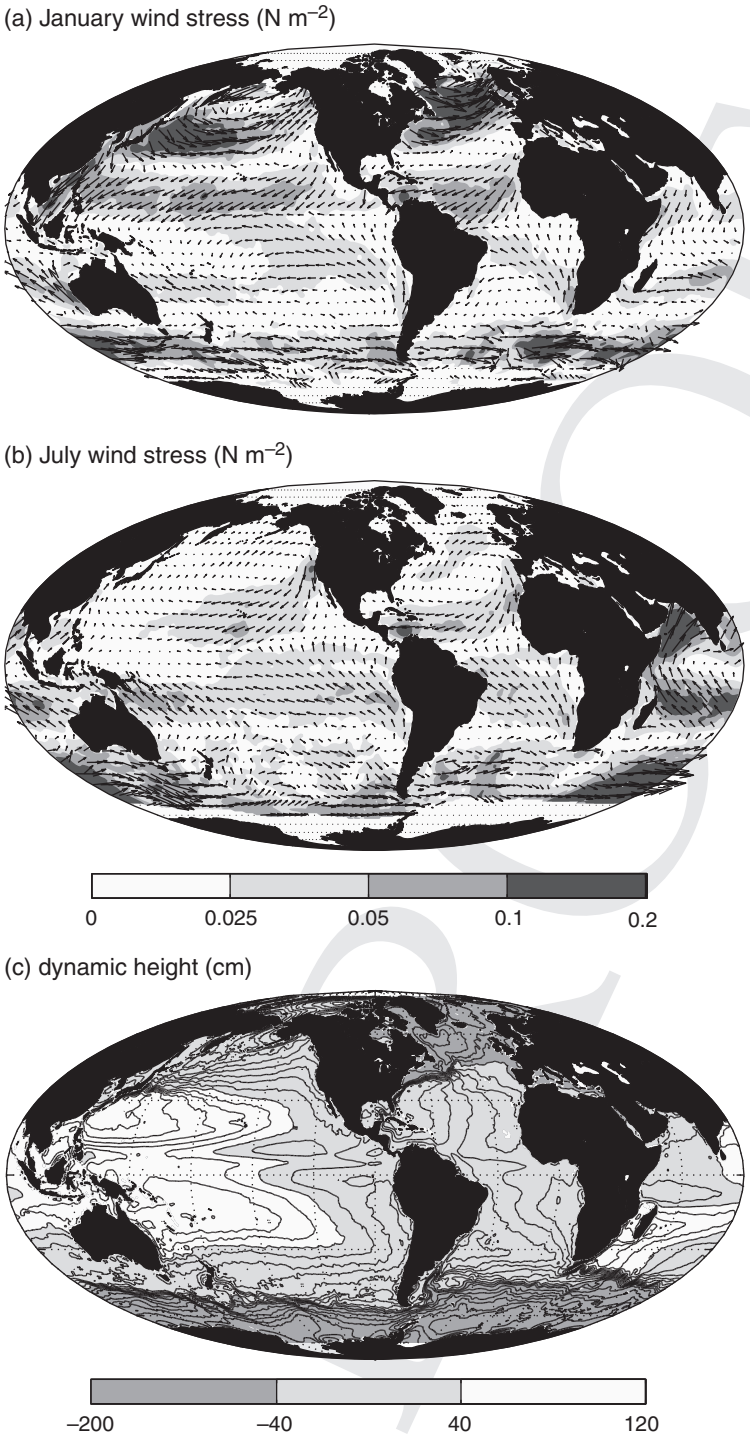

Figure 4.13 Global maps of surface-wind stress (N m^{-2}) for (a) January and (b) July from the NOCS climatology (Josey *et al.*, 2002), with (c) ocean mean dynamic height (contours with an interval of 10 cm and increased to 20 cm over the Southern Ocean); dynamic height details are given in Fig. 4.5 (Niiler *et al.*, 2003; Maximenko and Niiler, 2005). There is a much stronger wind-stress forcing (darker shading) in the winter hemisphere, reflecting the effect of the overlying jet stream and the pole–equator temperature gradient being stronger in winter. The surface geostrophic flow is aligned along dynamic height contours with high dynamic height to the right of the motion in the northern hemisphere.

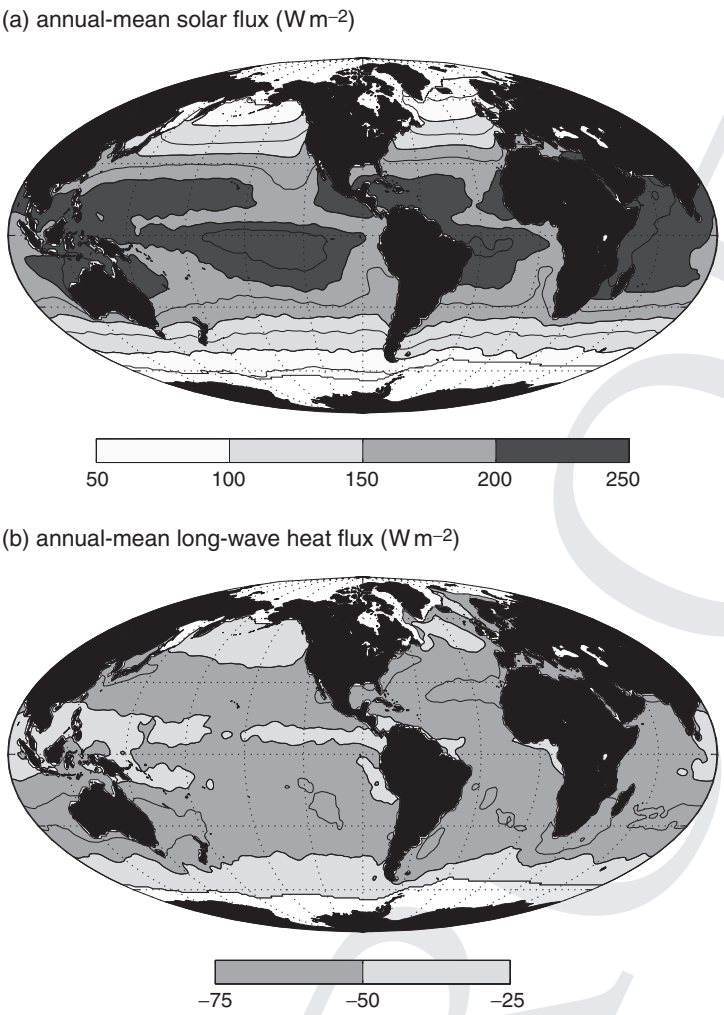

Figure 4.14 Annual-mean surface maps of (a) net solar heat flux from incoming minus reflected (contours every 25 W m^{-2}), and (b) net long-wave or infrared heat flux from incoming minus outgoing (contours every 12.5 W m^{-2}) from the NOCS climatology (Josey *et al.*, 1999). Positive values represent a heat flux into the ocean and polar regions have no data (white).

4.4.2 Air–sea exchange of heat

The surface heat flux into the ocean has several components,

$$\mathcal{H} = \mathcal{H}_{solar} + \mathcal{H}_{long} + \mathcal{H}_{latent} + \mathcal{H}_{sensible}, \qquad (4.12)$$

where the heat flux is defined by rate of energy supply per unit area, so the units are in energy per unit area and time, J m^{-2} s^{-1} = W m^{-2}, and the subscript identifies each component. The solar component, $\mathcal{H}_{solar}$, represents the radiative heat flux from the incoming solar radiation minus that reflected. This net solar heat input at the sea surface ranges from 250 W m^{-2} in the tropics to 50 W m^{-2} over the high latitudes when averaged over the year (Fig. 4.14a). This differential solar heating over the globe is the powerhouse of the atmosphere and ocean, driving a physical circulation that redistributes heat over the globe. The long-wave component, $\mathcal{H}_{long}$, represents the radiative heat flux over the range of wavelengths emitted from the sea surface, dominated by infrared radiation; the sign is again defined by incoming minus outgoing radiation, so that $\mathcal{H}_{long}$ is negative. The net outgoing long-wave radiation, $\mathcal{H}_{long}$, typically only reaches from −25 to −75 W m^{-2} (Fig. 4.14b), much smaller than the net solar heat input.

Hence, the radiative flux from the sum of these two components, $\mathcal{H}_{solar} + \mathcal{H}_{long}$, is directed into the ocean, varying from nearly 200 W m^{-2} in the tropics to less than 50 W m^{-2} at high latitudes

P1: SFK Trim: 246mm × 189mm Top: 7.5mm Gutter: 20mm
CUUK1441-04 CUUK1441/Williams 978 0 521 84369 0 May 20, 2011 20:34

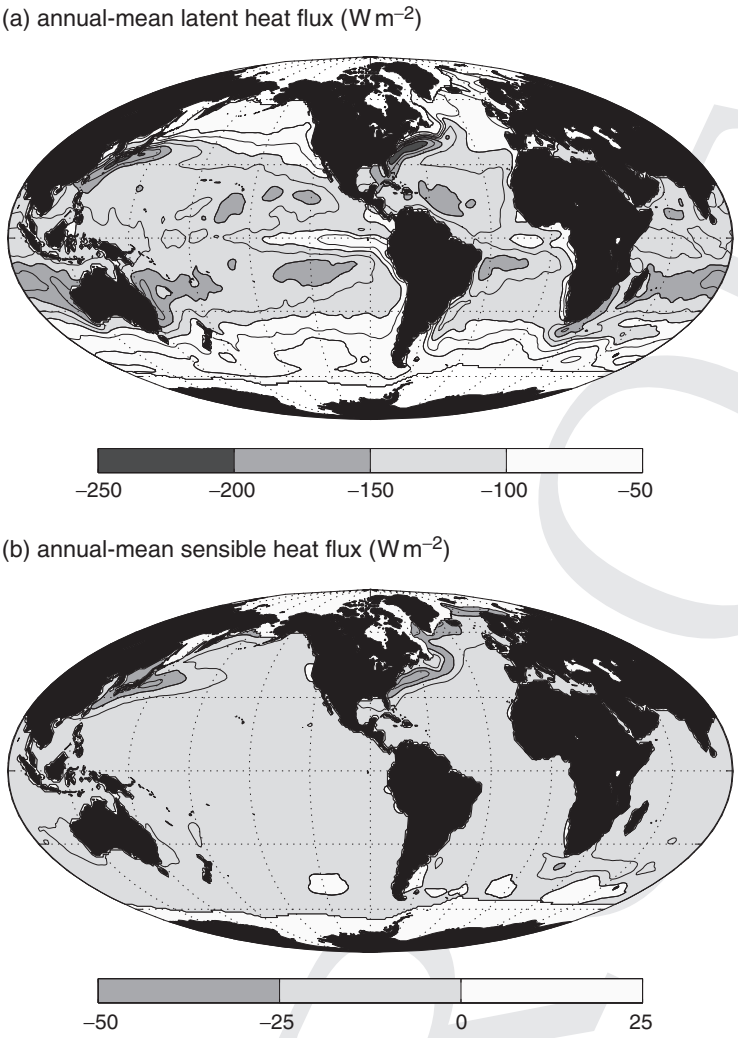

Figure 4.15 Annual-mean surface maps of (a) latent heat flux (contours every 25 W m^{-2}), and (b) sensible heat flux (contours every 12.5 W m^{-2}) from the NOCS climatology (Josey *et al.*, 1999). These negative values represent a heat transfer from the ocean to the atmosphere.

(Fig. 4.14). The radiative heating broadly decreases with latitude, but is modified by cloud cover with enhanced heat input occurring north and south of the equator, where there is reduced cloud cover.

This overall radiative heat input into the ocean is offset by the air–sea transfer of heat achieved through the sensible and latent contributions, $\mathcal{H}_{sensible} + \mathcal{H}_{latent}$ (each shown in Fig. 4.15). The air–sea heat flux by sensible heat is achieved by a turbulent transfer of heat across the sea surface depending on the air–sea temperature differences, while the latent heat flux is achieved by a turbulent transfer of evaporated water, where heat is used to enable the phase change from a liquid to a vapour. Stronger winds increase the surface cooling and evaporation from the ocean.

The latent exchange nearly always dominates over the sensible exchange, reflecting how much heat is stored and utilised in the phase changes of water. The sum of the sensible and latent heat fluxes varies typically from $-250\,\mathrm{W\,m^{-2}}$ to $-50\,\mathrm{W\,m^{-2}}$ (Fig. 4.15). This air–sea heat loss has a more complicated pattern than the radiative heat input. The maximum heat loss is over the western boundary currents, which is affected by how dry and cold is the air swept from the land relative to the warm ocean. Conversely, the minimum heat loss to the atmosphere is often far from the land, either in the Southern Ocean or the eastern side of

P1: SFK Trim: 246mm × 189mm Top: 7.5mm Gutter: 20mm
CUUK1441-04 CUUK1441/Williams 978 0 521 84369 0 May 20, 2011 20:34

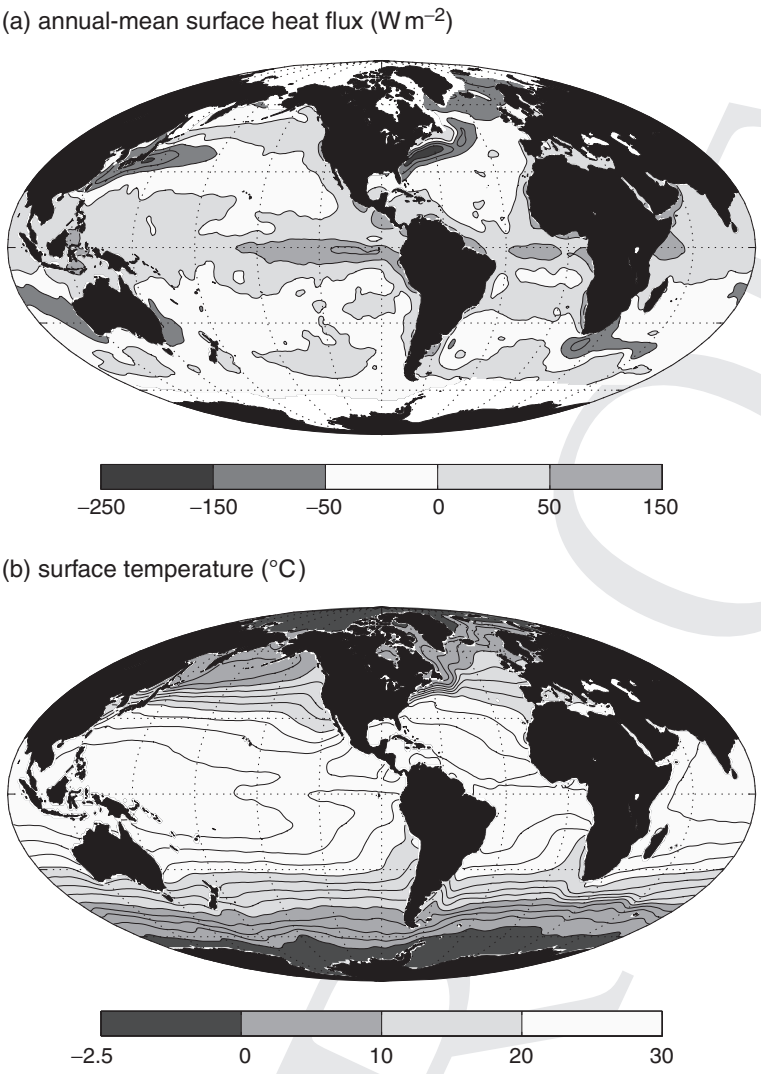

Figure 4.16 Map of (a) annual-mean, air–sea heat flux (contours every 50 W m^{-2}) into the ocean from the NOCS climatology (Josey *et al.*, 1999) and (b) sea-surface temperature (contours every 2.5 °C) from the *World Ocean Atlas 2001* (Conkright *et al.*, 2002). There are significant uncertainties in this net heat flux, perhaps ranging from 10% to 20% for each component making up the net flux.

the basins, where the air–sea contrasts in humidity and temperature are smaller.

In summary, at the sea surface, the warming of the ocean by solar heating is opposed by cooling from long-wave radiation and latent and sensible heat fluxes to the atmosphere. This upward heat flux warms the atmosphere and heat is transferred upward through the atmosphere by a combination of long-wave radiation and convection. At the top of the atmosphere, the outgoing long-wave radiation then balances the net incoming solar radiation when integrated over a year and the entire surface area of the planet.

Air–sea heat flux and surface temperature

The net surface heat flux, $\mathcal{H}$, into the ocean is defined by the sum of the warming from the solar heat input and cooling from the combination of long-wave radiation, latent and sensible heat exchange. There is *not* a local heat balance and, instead, there is a gain in heat over the expansive area of the tropics of typically 50 W m^{-2} versus a more localised loss of heat at high latitudes and over the western boundaries at mid latitudes, reaching −250 W m^{-2} (Fig. 4.16a). These heat fluxes drive a corresponding temperature change over a surface mixed layer of thickness

P1: SFK Trim: 246mm × 189mm Top: 7.5mm Gutter: 20mm
CUUK1441-04 CUUK1441/Williams 978 0 521 84369 0 May 20, 2011 20:34

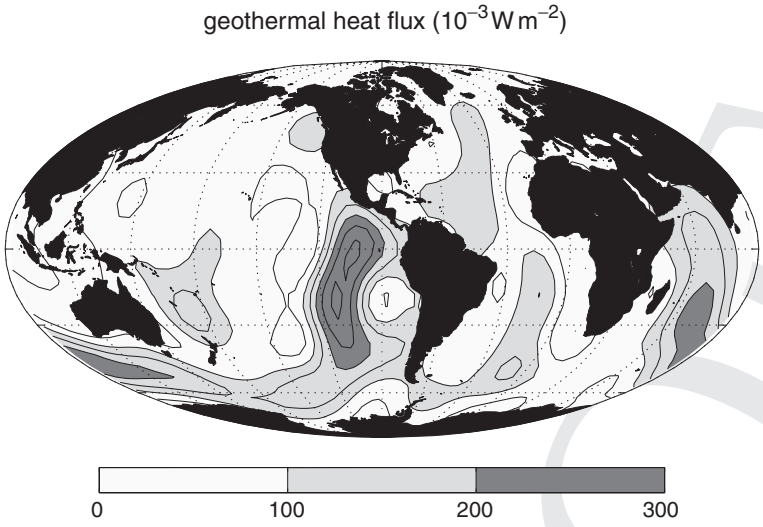

Figure 4.17 Geothermal heat flux at the sea floor (contours every 50×10^{-3} W m^{-2}). The heat flux is small and positive, acting continuously to warm the bottom waters. The estimate of geothermal heating is based on direct observations over the globe (with very few data in the Southern Ocean), which is then mapped with spherical harmonics on a 5° grid; replotted from Pollack *et al.* (1993) using data from http://www.ngdc.noaa.gov/Data.

h given by,

$$\frac{DT}{Dt} = \frac{1}{\rho C_p}\frac{\mathcal{H}}{h}, \tag{4.13}$$

where for simplicity any penetration of heat below the mixed layer is ignored, as well as entrainment or mixing; C_p is the heat capacity for seawater at a constant pressure in J kg K^{-1}. The surface heat flux is measured in W m^{-2}, so the units on each side of (4.13) are the same and given by

$$\frac{\mathrm{K}}{\mathrm{s}} = \frac{(\mathrm{J\,s^{-1}\,m^{-2}})}{(\mathrm{kg\,m^{-3}})(\mathrm{J\,kg^{-1}\,K^{-1}})(\mathrm{m})}.$$

At mid latitudes, the boundary currents provide a poleward transport of warm water leading to a westward increase in sea-surface temperature, while at high latitudes, the boundary currents provide an equatorward transport of cold water leading to a westward decrease in sea-surface temperature (Fig. 4.16b).

The annual gain in heat in the tropics and loss at high latitudes is generally offset by an ocean heat transport, directed poleward in the global average. However, the exception to this general rule is in the Atlantic, where the heat transport is directed northward even in the southern hemisphere: cold, deep water is transported southward and warm, surface water is transported northward over the entire basin, as part of the overturning circulation.

Geothermal heat flux from the sea floor

While the surface heat flux is the most important thermal forcing for the ocean, there is also a much smaller geothermal heating from the sea floor typically reaching 0.1 W m^{-2} (Pollack *et al.*, 1993). This geothermal heating is supplied by conduction from the lithosphere and is enhanced over topographic ridges (Fig. 4.17), particularly where there is hydrothermal activity. While this geothermal heat flux is several orders of magnitude smaller than the surface heat flux, the heat flux along the sea floor is always unidirectional, acting to warm the bottom waters and reduce their stratification.

4.4.3 Air–sea freshwater flux and surface salinity

Salinity, defined by the concentration of salt, is altered by the exchange of fresh water and salt with the atmosphere, land or ice: salt becomes more concentrated when there is a surface freshwater loss and, conversely, more diluted when there is a freshwater gain. Changes in the actual inputs of the salts are usually unimportant, apart from beneath ice sheets where ejection of salt during freezing leads to sinking plumes of dense, salty water.

Fresh water is exchanged between the atmosphere and ocean via precipitation, $\mathcal{P}$, and evaporation, $\mathcal{E}$ (Fig. 4.18a,b), as well as provided by river

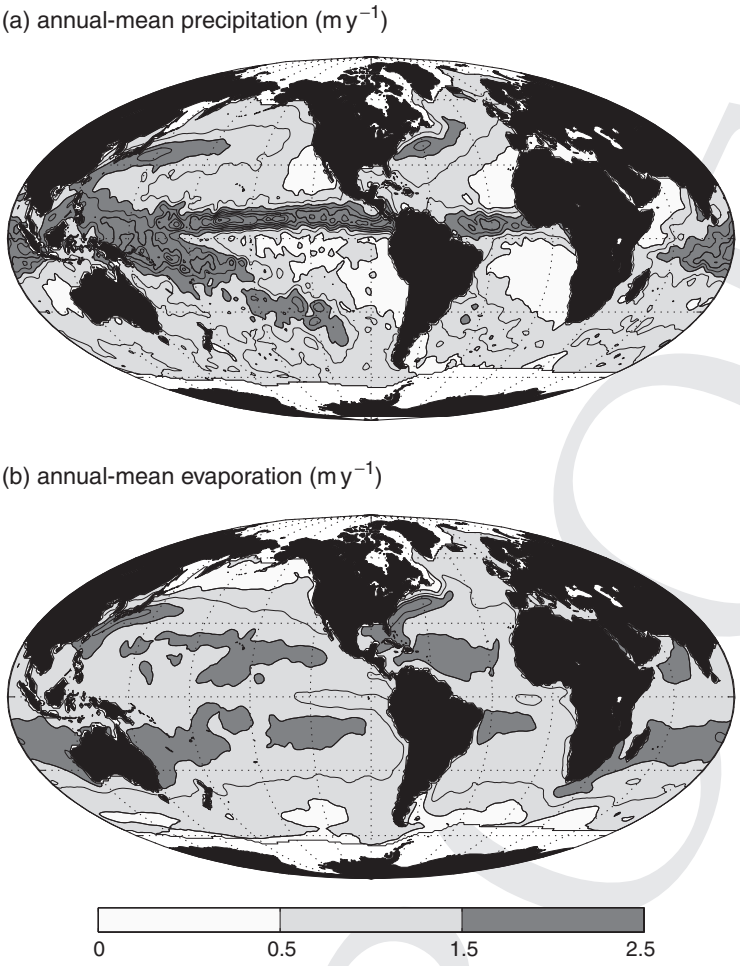

Figure 4.18 Maps of climatological, annual-average (a) precipitation into the ocean, and (b) evaporation out of the ocean (contours every 0.5 m y^{-1}) from the NOCS climatology (Josey *et al.*, 1999) with larger magnitudes denoted by dark shading.

run-off from land and exchanged through melting and freezing of ice; the units for the air–sea freshwater flux are given as m y^{-1} from the volume flux of fresh water (m^3 y^{-1}) exchanged per unit horizontal area (m^2). There is an overall input of fresh water to the ocean along a narrow band in the tropics, a loss of fresh water in the subtropics and an input of fresh water at mid and high latitudes (Fig. 4.19a).

The pattern of air–sea exchange of fresh water is rather more complicated than that for heat. The air–sea exchange of fresh water is controlled by (i) how precipitation increases with vertical ascent in the atmosphere, as seen along the inter-tropical convergence zone in the tropics and the atmospheric storm belts at mid latitudes (Fig. 4.18a), and (ii) how evaporation increases in warmer waters in the mid latitudes and where relatively dry air passes from the continents over the warm, ocean boundary currents (Fig. 4.18b).

A transfer of fresh water from the ocean to the atmosphere increases the concentration of salts and dissolved matter remaining in surface ocean, as measured by the salinity (Fig. 4.19b),

$$\frac{DS}{Dt} = S\frac{(\mathcal{E} - \mathcal{P})}{h}, \tag{4.14}$$

where the surface ocean is assumed to be well mixed over a thickness h and ignoring entrainment and mixing. If salinity is measured in g kg^{-1} and the freshwater fluxes as a volume flux per unit area in m^3 s^{-1} m^{-2}, then the units of each side of (4.14) are identical,

$$\frac{\text{g kg}^{-1}}{\text{s}} = (\text{g kg}^{-1})\frac{(\text{ m}^3\,\text{s}^{-1}\,\text{m}^{-2})}{(\text{ m})}.$$

P1: SFK Trim: 246mm × 189mm Top: 7.5mm Gutter: 20mm
CUUK1441-04 CUUK1441/Williams 978 0 521 84369 0 May 20, 2011 20:34

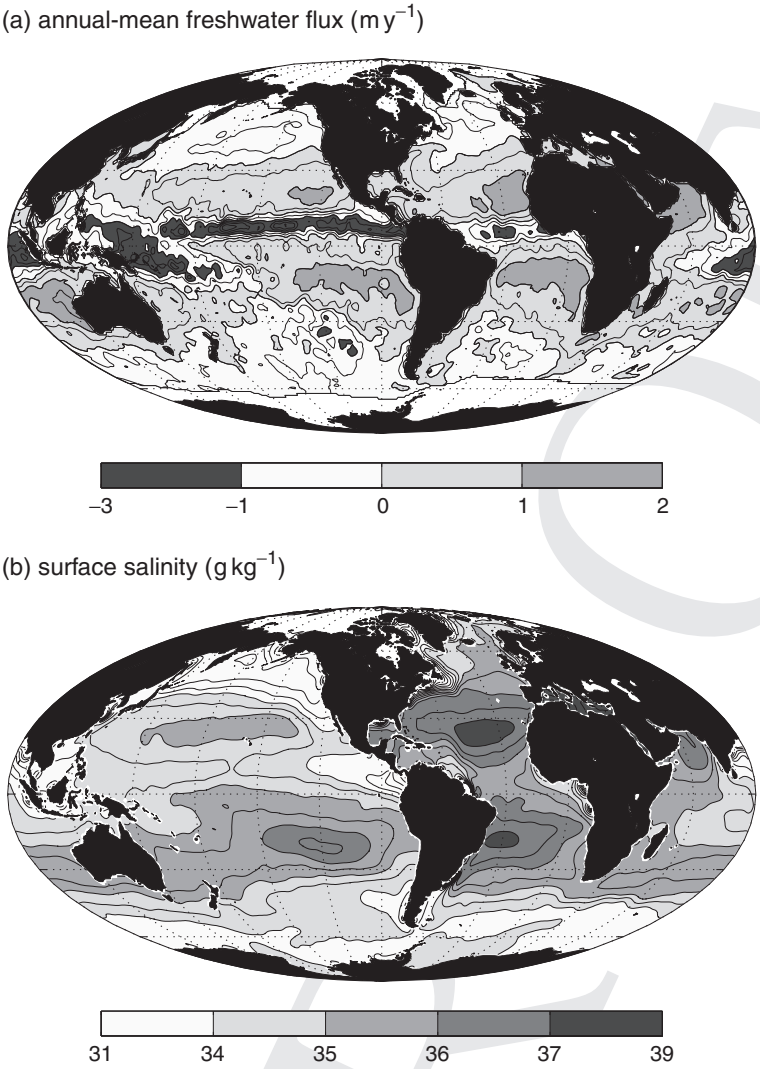

Figure 4.19 Maps of climatological, annual-average (a) freshwater flux out of the ocean (contours every 0.5 m y^{-1}) from the NOCS climatology (Josey *et al.*, 1999), shading emphasises extremes, positive flux is dark, negative is light, and (b) sea-surface salinity (contours every 0.5 g kg^{-1}) from the *World Ocean Atlas 2001* (Conkright *et al.*, 2002). There are significant uncertainties in this net freshwater flux, perhaps ranging from 10% to 20% for each component making up the net flux.

The annual-mean salinity is highest in concentration in low-latitude, semi-enclosed seas, such as the Mediterranean and the Red Sea, where evaporation is strong over warm waters and there is relatively little precipitation. Over the open ocean, salinity is relatively low in concentration along the tropics where precipitation is strong, then becomes greater over the subtropics reflecting a loss of fresh water from both enhanced evaporation and lack of precipitation (Fig. 4.19a,b). Salinity then weakens poleward at mid and high latitudes reflecting the effect of increased freshwater input from precipitation and ice melt (Fig. 4.19a,b).

The Pacific is much fresher than the Atlantic through an overall freshwater gain over the Pacific compared with the Atlantic, which is partly a consequence of enhanced precipitation over the tropical Pacific and enhanced evaporation over the subtropical Atlantic; this is discussed further in Chapter 12.

4.4.4 Air–sea forcing of surface density

The combination of the surface heat and freshwater fluxes alters the surface density: warming or freshening acts to lighten surface waters, while cooling or evaporation acts to increase the surface density. The forcing of surface density, $\mathcal{D}$,

P1: SFK Trim: 246mm × 189mm Top: 7.5mm Gutter: 20mm
CUUK1441-04 CUUK1441/Williams 978 0 521 84369 0 May 20, 2011 20:34

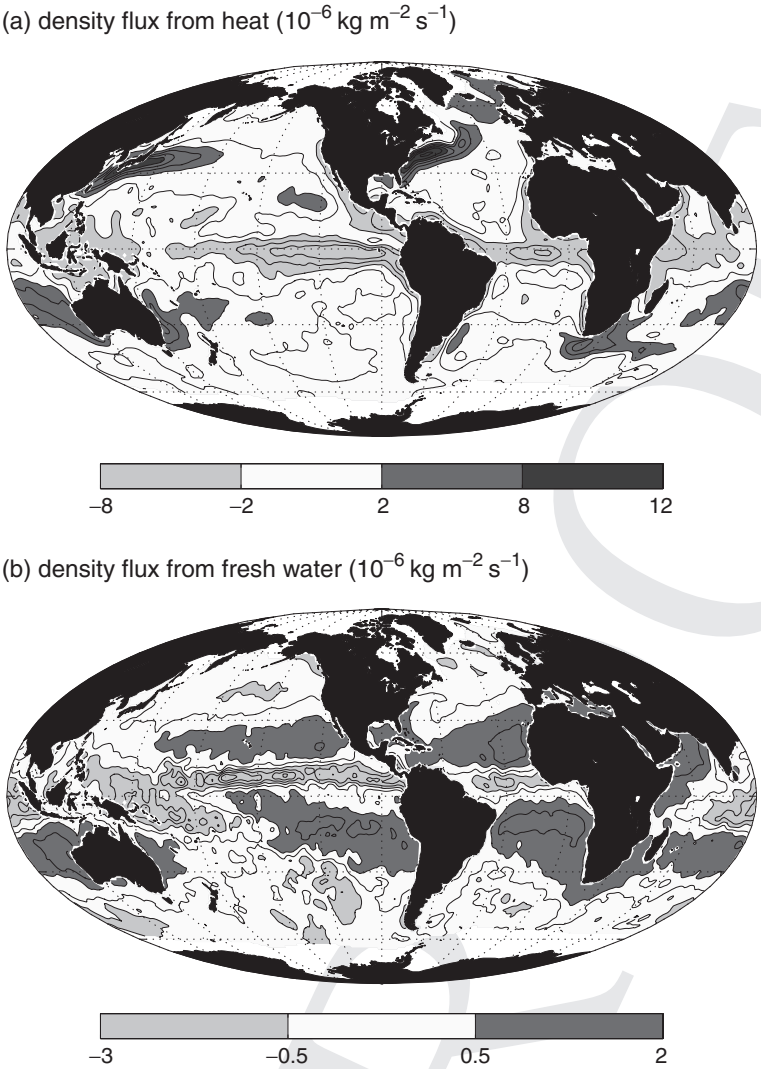

Figure 4.20 Maps of the contribution to the climatological, surface density forcing, $\mathcal{D}$, from (a) surface heat fluxes, $-\frac{\alpha_T}{C_p}\mathcal{H}$ (contours every 2×10^{-6} kg m^{-2} s^{-1}), and the weaker contribution from (b) surface freshwater fluxes, $\rho\beta_S S(\mathcal{E} - \mathcal{P})$ (contours every 0.5×10^{-6} kg m^{-2} s^{-1}), which are evaluated monthly using air–sea fluxes from NOCS (Josey *et al.*, 1999) and temperature and salinity from the *World Ocean Atlas 2001* (Conkright *et al.*, 2002). Note that the range is four times larger in (a) than in (b), and the shading is chosen to identify extremes for surface density input (dark) or loss (light).

can be defined in terms of the density effects of the surface heat and and freshwater fluxes given by

$$\mathcal{D} = -\frac{\alpha_T}{C_p}\mathcal{H} + \rho\beta_S S(\mathcal{E} - \mathcal{P}), \tag{4.15}$$

where $\mathcal{D}$ has units of mass per unit area and unit time, kg m^{-2} s^{-1}; α_T is the density expansion coefficient for temperature and β_S is the density contraction coefficient for salinity from the linearised equation of state (4.11); this surface forcing is often equivalently written in terms of a buoyancy flux, given by $-g\mathcal{D}/\rho$ with units of m^2 s^{-3}.

The surface density forcing is mainly provided by surface heat fluxes (Fig. 4.20a) and there is a smaller contribution by a factor of four or more from freshwater fluxes (Fig. 4.20b, note different scale). Evaporation leads to an increase in density over the central part of the subtropical gyre with $\mathcal{D} \sim 1 \times 10^{-6}$ kg m^{-2} s^{-1}, while the precipitation over the equator leads to a lightening of -2×10^{-6} kg m^{-2} s^{-1}. The freshwater contribution only becomes comparable to the thermal forcing over the eastern sides of ocean basins outside the tropics, as well as the Southern Ocean (Fig. 4.20b).

The relative importance of a thermal perturbation versus a saline perturbation in forcing density changes varies over the global ocean. To understand this variation, consider how

P1: SFK Trim: 246mm × 189mm Top: 7.5mm Gutter: 20mm
CUUK1441-04 CUUK1441/Williams 978 0 521 84369 0 May 20, 2011 20:34

Table 4.2 Variation of density expansion coefficients, $\alpha_T = -\frac{1}{\rho}\frac{\partial \rho}{\partial T}$ and $\beta_S = \frac{1}{\rho}\frac{\partial \rho}{\partial S}$, with temperature and pressure for a fixed salinity of 35 g kg^{-1}; evaluated from CSIRO SEAWATER library.

Temperature T (°C)	Pressure P (mbar)	Ratio of expansion coefficients α_T/β_S
20	0	0.3466
10	0	0.2198
5	0	0.1472
5	2000	0.2117
5	4000	0.2748

fractional density changes, $\Delta\rho$, from (4.11) are related to temperature and salinity changes, ΔT and ΔS, by

$$\frac{\Delta\rho}{\rho} = -\alpha_T \Delta T + \beta_S \Delta S,$$

where the relative contributions of ΔT and ΔS are measured by α_T and β_S. For given temperature and salinity changes, their relative importance in forcing density changes varies according to the ratio, α_T/β_S, which varies strongly with temperature, as well as pressure (Table 4.2). For the same temperature perturbation, the resulting density change in warm waters is twice as large as that induced in cold polar waters; conversely, a salinity perturbation becomes more important in controlling density changes in cold waters.

How might the evolution of thermal and freshwater anomalies differ?

While thermal forcing is generally more important in determining the surface density than freshwater forcing, there are some important subtleties. Thermal anomalies in the surface ocean can easily become dampened by air–sea interaction: a warm surface anomaly increases the local heat loss to the atmosphere from long-wave, latent and sensible heat loss. Hence, a warm surface anomaly cools more rapidly than its neighbouring environment, so that the surface anomaly can be dampened and removed; conversely, a cool, surface anomaly preferentially warms and again is damped. Ultimately, the importance of this air–sea damping varies with the horizontal scale of the anomaly: the atmosphere can easily dampen surface temperature signals associated with ocean eddies on scales of tens of kilometres over several weeks or months, but this damping is less rapid for ocean anomalies on much larger horizontal scales.

In contrast, freshwater or salinity anomalies are not dampened by air–sea interaction: a surface increase in salinity does not directly alter the air–sea flux of fresh water. Hence, once a salinity anomaly is formed in the surface ocean, the salinity anomaly can persist for much longer than a thermal anomaly; indeed, it is for this very reason that salinity is a very useful tracer, identifying the origin of water-mass properties.

Over the global scale, contrasts in freshwater forcing turn out to be very important in leading to different surface density conditions between different ocean basins, leading to contrasting overturning circulations in the North Atlantic and North Pacific (Section 12.1.3).

4.5 Summary

The physical balances operating in the ocean and atmosphere are more unintuitive than one might initially expect. The ocean moves in response to external accelerations involving gravity, contrasts in pressure and frictional stresses, as well as in response to two apparent accelerations, the centrifugal and Coriolis, depending on the rotation of the Earth. The centrifugal acceleration is an outward acceleration deforming the shape of the Earth from a perfect sphere to an ellipsoid. The Coriolis acceleration provides a deflection, directed to the right of the motion in the northern hemisphere and to the left in the southern hemisphere. This Coriolis effect is revealed in how atmospheric cyclones spin in an anticlockwise manner in the northern hemisphere and in a clockwise manner in the southern hemisphere. Despite popular myth, how water drains around a plug hole is not a reliable indicator, as the timescale is too short for the Coriolis acceleration to be significant.

The dominant physical balances for the ocean circulation turn out to be very different in the vertical and horizontal. In the vertical, gravitational

P1: SFK Trim: 246mm × 189mm Top: 7.5mm Gutter: 20mm
CUUK1441-04 CUUK1441/Williams 978 0 521 84369 0 May 20, 2011 20:34

acceleration is balanced by vertical pressure contrasts, with pressure increasing with depth given the increasing weight of overlying fluid. In the horizontal, there is a three-way balance between Coriolis acceleration, horizontal pressure gradients and frictional stresses. The Coriolis acceleration acts to deflect the flow such that fluid either moves parallel to pressure contours or perpendicular to frictional stresses. This three-way balance is usually separated into a geostrophic balance between the Coriolis acceleration and the pressure gradient, together with an Ekman balance confined close to the surface and sea floor between the Coriolis acceleration and the frictional stress.

The effect of the Coriolis acceleration is very profound. Away from boundaries, fluid does not simply move from high to low pressure, but rather along pressure contours. Since the pressure contrasts driving the flow are not easily removed, flows tend to keep moving and, hence, the ocean and atmosphere are full of persistent currents and jets! Eventually, frictional stresses at the surface and bottom boundaries do become important and the atmospheric and ocean flows become damped, but the rate at which these currents spin down is much slower than one might initially expect.

The ocean circulation is primarily forced by this movement of the atmosphere via air–sea exchanges of momentum, heat and fresh water. The surface wind pattern provides the frictional forcing of the surface ocean, evident in the sense of rotation of the ocean gyres within the basins and the direction of the zonal currents in the tropics and the Southern Ocean. The surface heat flux leads to the expected surface temperature contrasts: warming in the tropics and cooling at high latitudes, apart from the surprise that the maximum surface cooling occurs over the western side of ocean basins where there are warm boundary currents. The surface freshwater flux has a more complex pattern: precipitation occurs where air is rising in the tropics or in mid-latitude weather systems, while evaporation increases where waters are warmer. The combination of the surface heat and freshwater forcing alters the surface density of the ocean; thermal contribution is usually the controlling factor, apart from at high latitudes where the freshwater contribution becomes increasingly important.

These physical concepts of how the ocean circulates are taken further in subsequent chapters addressing specific phenomena: how ocean gyres circulate, how ocean eddies form, how the ocean is ventilated and how the deep ocean circulates.

4.6 Questions

Q4.1. Apparent accelerations.

When particles are viewed in a rotating frame, they appear to be deflected by apparent accelerations. Consider the case of a particle initially moving only in the x-direction on the rotating Earth, which is deflected by the Coriolis acceleration. The particle travels a distance of 100 m in the x-direction in a time of either (i) 10 s or (ii) 10^4 s.

For each case, (a) calculate the Coriolis acceleration to the right of the motion in the y-direction given by $-fu$, where u is the zonal velocity in the x-direction and f is the Coriolis parameter; $f = 2\Omega \sin\phi$, where $\Omega = 2\pi/\text{day}$ and ϕ is the latitude, which assume here is at 30°N.

(b) calculate the displacement in the y-direction using $s = \frac{1}{2}at^2$ from the Coriolis acceleration, where s is the displacement, a is the Coriolis acceleration in the y-direction, and t is time.

(c) Comparing the x and y displacements, calculate the angle of flight (relative to the initial path).

(d) Compare your answers for (i) and (ii), and discuss in which cases the Coriolis effect appears to be more important.

(e) How might the situation change in the southern hemisphere?

Q4.2. Thermal-wind balance across the Antarctic Circumpolar Current.

Thermal-wind balance relates the vertical shear in geostrophic velocity to the horizontal density gradient, which for the eastward flow is given by

$$\frac{\partial u}{\partial z} = \frac{g}{\rho f}\frac{\partial \rho}{\partial y}.$$

(a) Derive thermal-wind balance by differentiating geostrophic balance (4.5a) with depth and substituting hydrostatic balance (4.2).

P1: SFK Trim: 246mm × 189mm Top: 7.5mm Gutter: 20mm
CUUK1441-04 CUUK1441/Williams 978 0 521 84369 0 May 20, 2011 20:34

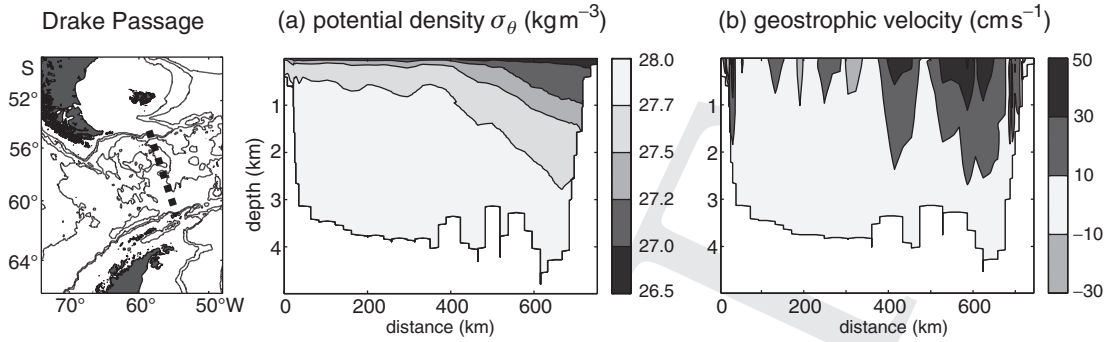

Figure 4.21 Section through Drake Passage between South America and Antarctica in the Southern Ocean for (a) potential density referenced to the sea surface minus 1000 kg m^{-3}, σ_θ, and (b) eastwards geostrophic velocity (cm s^{-1}), relative to an assumed zero flow on the sea floor versus depth together with a map of bathymetry and position of section (dashed line) in the left panel. The distance along the section increases northward. Data collected between 30 December 1997 and 7 January 1998 with a maximum station spacing of 17 km. Data supplied by Brian King; for further details, see Cunningham *et al.* (2003).

(b) Consider the density variations across the Drake Passage in the Southern Ocean (Fig. 4.21). Estimate the change in eastward velocity, Δu_g, associated with the northward change in density, $\Delta\rho$, over a depth scale Δz using a differenced-version of thermal wind,

$$\Delta u_g \sim \frac{g}{\rho f}\frac{\Delta\rho}{\Delta y}\Delta z.$$

Take $\Delta\rho$ from Fig. 4.21a over a north–south distance $\Delta y \sim 300$ km and a depth change $\Delta z \sim 2$ km with $f \sim -10^{-4}$ s^{-1}. Check the units and sign of your answer. Compare your answer to the observed geostrophic velocity in Fig. 4.21b.

Q4.3. Scaling of terms in the momentum equation for a Gulf Stream ring.

(a) Consider the flow associated with an ocean eddy formed by the meandering of the Gulf Stream. Assume that the typical magnitude for the current speed is given by $U \sim 0.5$ m s^{-1} and a horizontal length scale $L \sim 100$ km and vertical height scale $H \sim 500$ m, then estimate (i) the advective timescale given by L/U; and (ii) an upper bound for the vertical velocity from $W < UH/L$.

(b) The x-component of the unforced, momentum equation (4.1a) is given by

$$\frac{Du}{Dt} - 2\Omega v\sin\phi + 2\Omega w\cos\phi + \frac{1}{\rho}\frac{\partial P}{\partial x} = 0.$$

Crudely estimate the magnitude of the first three terms, assuming that the rate of change following the motion is typically given by $Du/Dt \sim U^2/L$, the horizontal velocities are $u \sim v \sim U$ and the vertical velocity $w \sim W$; assume the angular velocity $\Omega = 2\pi/86\,400$s and a latitude $\phi \sim 35°$N.

Hence, identify which term balances the horizontal pressure gradient.

(c) Show how the relative importance of the temporal acceleration and the Coriolis acceleration is given by the non-dimensional Rossby number,

$$Ro = \frac{U}{fL}.$$

Calculate how large the Rossby number is for the ocean ring.

Q4.4. Divergence and curl.

(a) For the velocity fields for a circulating flow and a reversing jet, depicted in Fig. 4.22, speculate on whether there is (i) any horizontal divergence, i.e., whether more fluid leaves a unit area than enters the unit area (where more fluid leaving a region is defined as positive divergence), and (ii) any rotation of the velocity field, i.e., defined by how a paddle wheel placed in the flow will rotate (where an anticlockwise rotation is defined as a positive rotation). In each case, identify the sign of your answer.

(b) More formally, now evaluate the horizontal divergence, $\frac{\partial u}{\partial x} + \frac{\partial v}{\partial y}$, and the relative vorticity measuring the rotation of the fluid, $\zeta = \frac{\partial v}{\partial x} - \frac{\partial u}{\partial y}$, corresponding to the velocity fields depicted in Fig. 4.22.

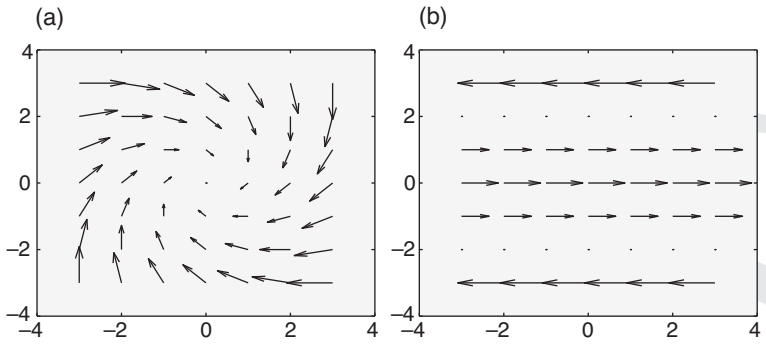

Figure 4.22 Velocity fields for (a) a circulating flow, and (b) a reversing jet. The horizontal divergence is denoted by whether more fluid leaves a horizontal area than enters it. The relative vorticity, ζ, is denoted by whether a paddle wheel placed in the flow rotates in an anticlockwise manner.

Assume that the eastward velocity, u, and northward velocity, v, vary in x and y in the following manner: (i) $u = y - x$ and $v = -x - y$; and (ii) $u = 2 - 0.5y^2$ and $v = 0$.

4.7 Recommended reading

There are a range of excellent and comprehensive texts which carefully discuss the equations of motion and derive the relevant balances:

B. Cushman-Roisin (1994). *Introduction to Geophysical Fluid Dynamics*. Englewood Cliffs, NJ: Prentice Hall, 320pp.

A. E. Gill (1982). *Atmosphere-Ocean Dynamics*. New York: Academic Press, 692pp.

J. Marshall and A. R. Plumb (2007). *Atmosphere, Ocean and Climate Dynamics.* Burlington, MA: Academic Press/Elsevier, 319pp.

J. Pedlosky (1987). *Geophysical Fluid Dynamics*. New York: Springer-Verlag, 710pp.

G. K. Vallis (2006). *Atmospheric and Oceanic Fluid Dynamics: Fundamentals and Large-Scale Circulation*. Cambridge: Cambridge University Press, 745pp.